Environmental Technology & Innovation 27 (2022) 102795

Contents lists available at ScienceDirect

Environmental Technology & Innovation

journal homepage: www.elsevier.com/locate/eti

New material of polyacrylic acid-modified graphene oxide composite for phenol remediation from synthetic and real wastewater

Amina Bibi [a], Shazia Bibi [b], Mohammed Abu-Dieyeh [b], Mohammad A. Al-Ghouti [a,*]

[a] Environmental Science Program, Department of Biological and Environmental Sciences, College of Arts and Sciences, Qatar University, Doha, P.O. Box: 2713, Qatar
[b] Biological Sciences Program, Department of Biological and Environmental Sciences, College of Arts and Sciences, Qatar University, Doha, P.O. Box: 2713, Qatar

ARTICLE INFO

Article history:
Received 12 April 2022
Received in revised form 9 June 2022
Accepted 27 June 2022
Available online 30 June 2022

Keywords:
Phenolic compounds
Adsorption
Graphene oxide
Polyacrylic acid

ABSTRACT

In this study, new material of polyacrylic acid-modified graphene oxide (GO-PAA) composite for phenol remediation from synthetic and real wastewater was investigated. The graphene oxide (GO) and GO-PAA were physically and chemically characterized using scanning electron microscopy (SEM), transmission electron microscopy (TEM), Fourier transform infrared spectroscopy (FTIR), energy dispersive X-ray analysis (EDX), and Brunauer–Emmet–Teller (BET). The effects of various experimental factors including pH, temperature, and initial phenol concentration were examined. Results showed that the optimum adsorption occurred at pH 2 and temperature 25 °C. The adsorption capacity of GO-PAA was double of the case of un-modified GO, indicating the importance of surface modification and the introduction of (C=O) groups in the enhancement of the adsorption process. Moreover, the Langmuir adsorption isotherm was found to be the most suitable isotherm to describe the adsorption process of phenol, and thermodynamics studies confirmed the spontaneity and the exothermic nature of the adsorption process. GO-PAA was capable of removing 75% and 18% of phenol from synthetic and real wastewater, respectively under optimum conditions of pH 2 and 25 °C. These results indicate that adsorption of phenolic compounds using GO-PAA could be an effective and simple method to remediate pollution, especially in acidic conditions.

1. Introduction

Phenolic compounds are a group of the many pollutants that are contaminating resources and decreasing the quality of water. Phenols are water-soluble organic compounds that consist of aromatic rings to which one or more hydroxyl (-OH) groups are attached. Phenolic compounds are either produced naturally or are released into the environment from various industries (Soto-Hernandez et al., 2017). The introduced phenolic compounds are considered persistent organic pollutants that are resistant to degradation through biological, chemical, and photolytic processes (Mohamed et al., 2020). As a consequence, phenol was categorized by the U.S. Environmental Protection Agency (US-EPA) as one of the 129 specific priority pollutants that are considered toxic and should be remediated (US-EPA, 2014). It is estimated

* Corresponding author.
E-mail address: mohammad.alghouti@qu.edu.qa (M.A. Al-Ghouti).

https://doi.org/10.1016/j.eti.2022.102795

that more than ten million tons of these compounds are released into the environment every year (Alshabib and Onaizi, 2019). Pharmaceutical, petrochemical, textile, leather, and agrochemical industries as well as industrial processes such as paper, pulp, paint, and pesticide production are the main sources of phenolic compound discharges (Deng et al., 2011). Proper handling of phenolic compounds is vital since they can adversely affect both human health and the environment. For humans, phenolic compounds can induce genotoxicity, carcinogenicity, muscle fatigue, metabolic disorders, bronchoconstriction, and dysfunction of the liver and kidneys. In the environment, phenolic compounds can contaminate soil, surface water bodies, and groundwater (Alshabib and Onaizi, 2019; Mohamad Said et al., 2021). Progressively, these compounds can induce changes in the structure of plant communities and accumulate in birds and fish, and eventually enter the food chains and cause adverse effects on human health (Garg et al., 2020; Mandeep and Kakkar, 2020). Therefore, phenolic compound concentrations in industrial effluents should not exceed 5 ppm if these discharges are to be directly ejected into public sewage systems. On the other hand, if these discharges are to be released into inland water bodies, the maximum permissible discharge level of phenolic is only 1 ppm. Moreover, according to the US-EPA, the level of phenolic compounds should not exceed 1 ppb in drinking water (Alshabib and Onaizi, 2019).

For example, olive mill wastewater (OMW) is considered one of the main problems faced by olive oil manufacturing companies, due to the presence of various pollutants at high concentrations (Mulinacci et al., 2001). It is estimated the annual world production of OMW is between 10 to 30 million m^3 (Rahmanian et al., 2014). Due to excessive washing required during the production of olive oil, large volumes of OMW are generated in the Mediterranean countries. OMW is characterized by low pH levels (2.2–5.9) and contains many organic pollutants including tannins, polyalcohol, sugars, proteins, pectins, fats, lipids, and high levels of phenols (Solomakou and Goula, 2021), and the concentration of phenolic compounds in wastewater could exceed 10 g/L (Azbar et al., 2004; Hamdi, 1993; Kissi et al., 2001; Mulinacci et al., 2001). Thus, eco-friendly, and economically feasible solutions are required to protect the environment from the effects of such effluents.

Removal of phenolic compounds from wastewater has been done previously using different physicochemical techniques, including distillation, chemical oxidation, reverse osmosis, filtration, extraction by solvents, photocatalytic degradation, and adsorption (Garg et al., 2020). However, each of these techniques has some drawbacks aside from their advantages. The disadvantages are mainly the high maintenance and operational costs, high energy demand, pretreatment requirements, inefficiency of treatment, scaling, fouling, limitation due to selectivity and pH level, and the use of solvents that are not eco-friendly (Gholami-Bonabi et al., 2020; Jiménez et al., 2018).

Adsorption is one of the common methods for phenol remediation. Over the years, significant efforts have been made to develop and produce adsorbents with high efficiency and selectivity, biocompatibility, environmental compatibility, and cost-efficiency. Many adsorbents are being studied, particularly in the field of water treatment due to their versatility, wide applicability, and benign nature (Thakur and Kandasubramanian, 2019). Recent studies showed that various adsorbents including activated carbon (Xie et al., 2020), fly ash (Oyehan et al., 2020), carbon nanotubes (Saleh et al., 2020), and biopolymer-based biochar (Li et al., 2019) were effective in the removal of phenol from wastewater. Adsorption is a simple, energy-efficient, and cost-effective process that can remove both low and high concentrations of various pollutants including phenolic compounds from wastewater. In addition, the recycling of the adsorbent material is also possible, making this technique more cost-effective (Sajid et al., 2018).

Graphene oxide (GO) was discovered in 2004, and since then many unique mechanical and electric properties have been studied and explored for this wonder material. In terms of structure, graphene has a hexagonal honeycomb crystal lattice structure with a thickness of just one atom. Remarkably, one suspended layer of graphene is considered one of the stiffest materials. Due to the lack of thickness, graphene can be characterized by its surface and any modification to the material can lead to significant changes in its properties (Tong and Loh, 2014). Graphene has a polyaromatic π-system that enables its interactions with organic entities in water, where the rings of graphene would stack with the rings of the organic pollutants by π–π stacking interaction or hydrophobic effects (Shi et al., 2016). However, due to graphene's hydrophobic nature, its application in water decontamination is limited (Thakur and Kandasubramanian, 2019). Graphene oxide (GO), which is a derivative of graphene but with a surface packed with active groups such as carbonyl (C=O), carboxylic (–COOH), hydroxyl (–OH), and epoxide (C–O–C), providing significant active sites for modification and creating polar surface properties (Aliyev et al., 2019b; Gholami-Bonabi et al., 2020). Oxygen functional groups of various species and amounts are sited on both sides of the basal plane of the GO particles (Eigler, 2021). However, on GO's nanosheets, the phenolic epoxy (C–O–C), and hydroxyl (=OH) groups are in the basal plane while the carboxylic (=COOH) groups are located at the edges (Aliyev et al., 2019a). Due to their properties, graphene oxide composites have been used in the adsorption of various pollutants, including many heavy metals such as arsenic (Das et al., 2020), gallium (Zhang et al., 2019), and lead (Hur et al., 2015), as well as numerous organic contaminants such as aniline (Fakhri, 2017), organic dyes (Molla et al., 2019) and polycyclic aromatic hydrocarbons (Sun et al., 2013).

Even though the inherent characteristics of graphene-based materials have been of significant importance in adsorption studies, however, surface modification of GO could further improve their properties, and in turn, enhance the adsorption capacity of such materials. Thus, in this study, GO was modified with polyacrylic acid (PAA) which is a polymer of acrylic acid with a carboxyl (C=O) group on every two carbon atoms of its main chain. In water, PAA becomes a polyelectrolyte through the dissociation of the acid groups, and when all the carboxyl groups are dissociated, PAA develops a high negative charge density (Terao, 2021). As mentioned, many researchers investigated the use of various adsorbents in the removal of phenolic compounds from wastewater. Many studies also investigated the use of graphene oxide, and composites in

the removal of phenol however, to the best of our knowledge; no reports are available regarding graphene oxide's surface modification with polyacrylic acid and its role in the improvement of the adsorption process and mechanisms. Therefore, this study will investigate and compare the capacity of the GO and GO-PAA adsorbents in the removal of phenol under different experimental conditions including pH, temperature, and initial phenol concentration from synthetic and real wastewater (olive mill wastewater (OMW)) samples.

2. Materials and methods

2.1. Materials

Graphite powder (−60 mesh), sulfuric acid (H_2SO_4), 95%, potassium permanganate ($KMnO_4$), 99%, phosphoric acid (H_3PO_4), 85%, and hydrogen peroxide (H_2O_2), 30% were purchased from "Research lab" company. Whereas hydrochloric acid (HCl), 35% to 38%, was purchased from Scharlu. N, N′-methylene-bis-acrylamide was purchased from Glentham life sciences.

2.2. Methodology

2.2.1. Graphene oxide synthesis using modified Hummers' methods

Graphene oxide was synthesized using the modified Hummers' method as illustrated in Fig. 1(A) and 1(B). Briefly, a mixture of 96 mL sulfuric acid H_2SO_4 (74.2 wt%) and 24 mL phosphoric acid H_3PO_4, (19.7 wt%) was mixed and stirred in an ice bath for a few minutes. Then, 4 g graphite (G) and 12 g $KMnO_4$ were added gradually into the mixing solution under continuous stirring. The reaction mixture was then moved to an oil bath at 95 ± 2 °C for 0.5 h under reflux conditions. Following that, 100 mL of distilled water (DW) was added, and the reaction mixture was kept stirring for another 0.5 h. Finally, the mixture was transferred back to the ice bath where the reaction was terminated by the addition of 300 mL of DW and 40 ml of H_2O_2. The prepared solution was then diluted using 20% HCl solution and then centrifuged at 5000 rpm for 0.5 h. The supernatant was then removed away, and the residual GO was washed several times with the DW until the pH became neutral. The prepared GO was dried in the oven at 60 °C for about 60 h (Alkhouzaam et al., 2020).

2.2.2. Modification of graphene oxide using polyacrylic acid (GO-PAA)

The functionalization of graphene oxide was done by in-situ polymerization. Briefly, 1.5 g of the previously prepared graphene oxide was dispersed in a mixed solvent of ethanol and water (1:1, 500 mL), and the mixture was continuously stirred for 1.5 h at room temperature using a magnetic stirrer. Following that, 25 mL of acrylic acid (AA), 0.1 g of N, N′-methylene bisacrylamide (MBA), and 0.5 g of potassium persulfate (KPS) were added to the mixture, the bottle was then covered with Parafilm, and it was stirred again at room temperature for 0.5 h under N_2 purging system. Consequently, the mixture was reacted in an oven at 80 °C for 5 h. The GO-PAA composite was centrifuged at 4000 rpm for 0.5 h, then washed with DW, and dried thoroughly at room temperature (Zhang et al., 2019).

2.2.3. Synthetic phenol water stock preparation

Phenol stock solution with a concentration of 100 mg/L was prepared by the addition of 0.1 g of phenol to (1 L) distilled water. Following that, samples with concentrations of (Blank, 1, 2, 3, 4, 5, 6, 7, 8, 9, 10, 20, 40, 60, 80, and 100) mg/L were prepared by diluting the stock solution to prepare and draw a standard curve. UV–Vis spectrophotometer (JENWAY) was utilized to determine the concentration of phenol in standard and non-standard samples, and the curve was drawn at 270 nm wavelength (Gholami-Bonabi et al., 2020).

2.2.4. Batch experiments

Batch adsorption experiments were carried out in 100 mL bottles with 20 mL phenol solutions of known concentration, to that 0.02 g of the GO and GO-PAA were added. The bottles were then placed at a constant agitation speed of (165 rpm) for 24 h using a rotary shaker (Brunswick Innova® 2100/2150). The pH adjustments were carried out using 0.1 M HCl and 0.1 M NaOH. The effects of several parameters were studied including pH (2, 4, 6, 8, and 10), the concentration of phenol solution (20, 30, 40, 50, 60, 70, 80, and 100 mg/L), and temperature (25 °C, 35 °C, and 45 °C). Following that, the samples were collected from the bottles and filtered using a syringe and filter (Ahlstrom 0.45 μm). The concentration of phenol was determined by ultraviolet–visible (UV–Vis) spectroscopy at the wavelength of 270 nm (JENWAY). All of the batch experiments had two replicates and the mean value was used for data analysis. Phenol removal (%) and adsorption capacity were calculated for each sample according to equations (1) and (2), respectively:

$$\text{Removal } (\%) = \frac{C_i - C_f}{C_i} * 100 \tag{1}$$

Where C_i and C_f are the initial and final concentrations (mg/L) of phenol in the solution.

$$\text{Adsorption capacity, } qe\,(\frac{mg}{g}) = \frac{(C_i - C_f) \times V}{W} \tag{2}$$

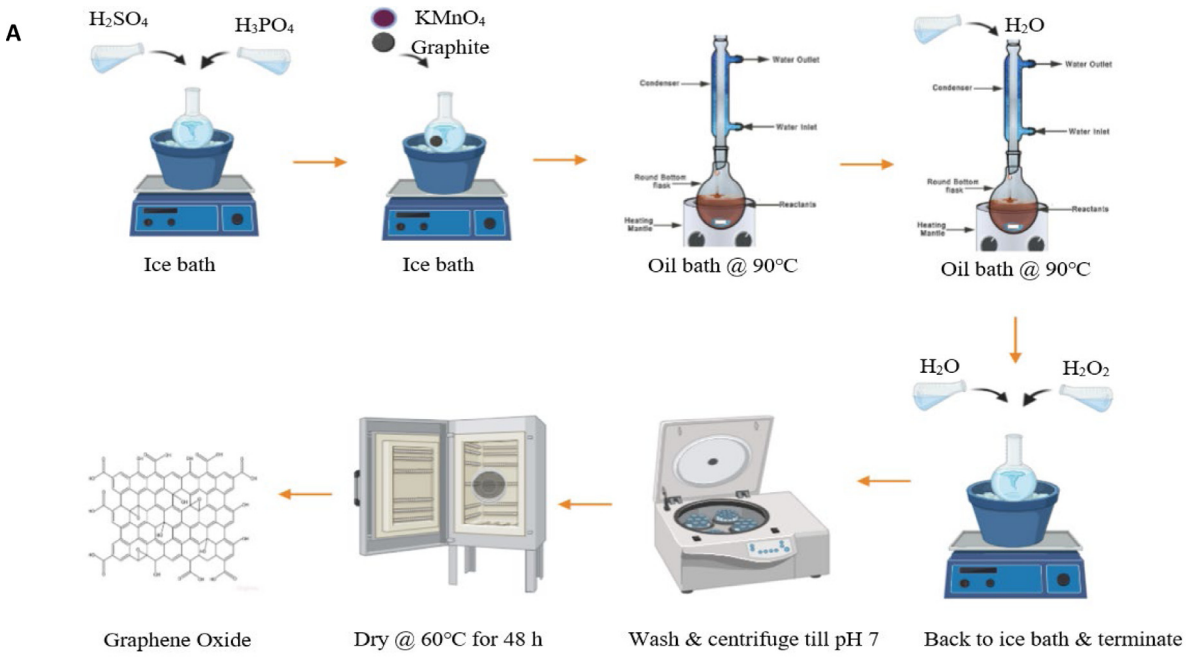

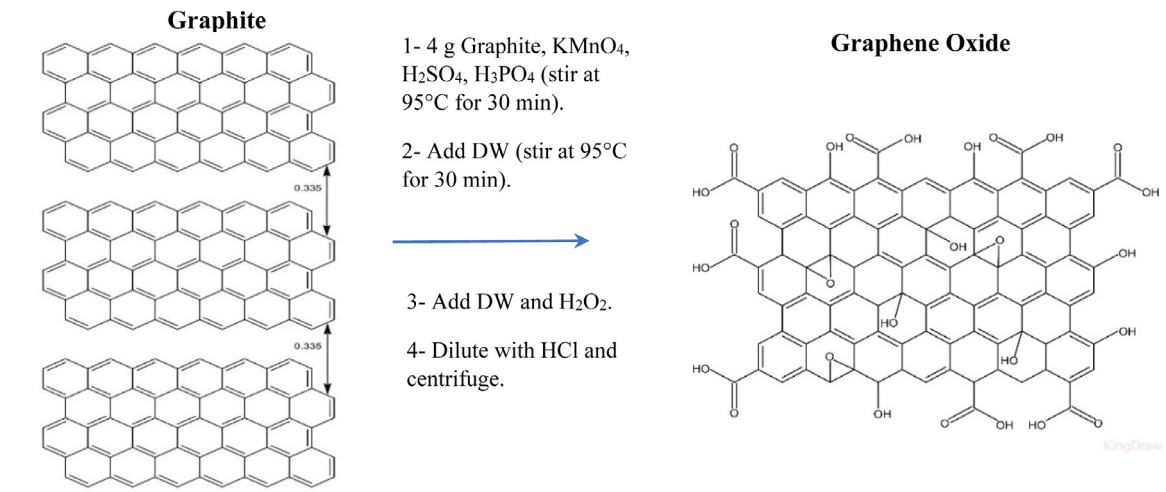

Fig. 1. (A) Graphene oxide synthesis using modified Hammers' methods, and (B) Reaction conditions for modified Hummers method (Adetayo and Runsewe, 2019; Alkhouzaam et al., 2020).

Where C_i and C_f are the initial and final concentration (mg/L) of phenol in the solution, V is the volume of solution (L) and W is the weight of adsorbent (g).

The batch adsorption was also carried out in duplicates for a real wastewater sample, which was olive wastewater. Since the wastewater sample was highly concentrated, adsorption was carried out at three different concentrations of wastewater (25%, 50%, and 100%), and it was done with and without pH adjustment.

2.2.5. Characterization of GO and modified GO-PAA

The prepared GO and GO-PAA were characterized using several physical and chemical techniques. Surface morphology and characterization of GO and GO-PAA were done using scanning electron microscopy (SEM) (Nova™ Nano SEM 50 Series)

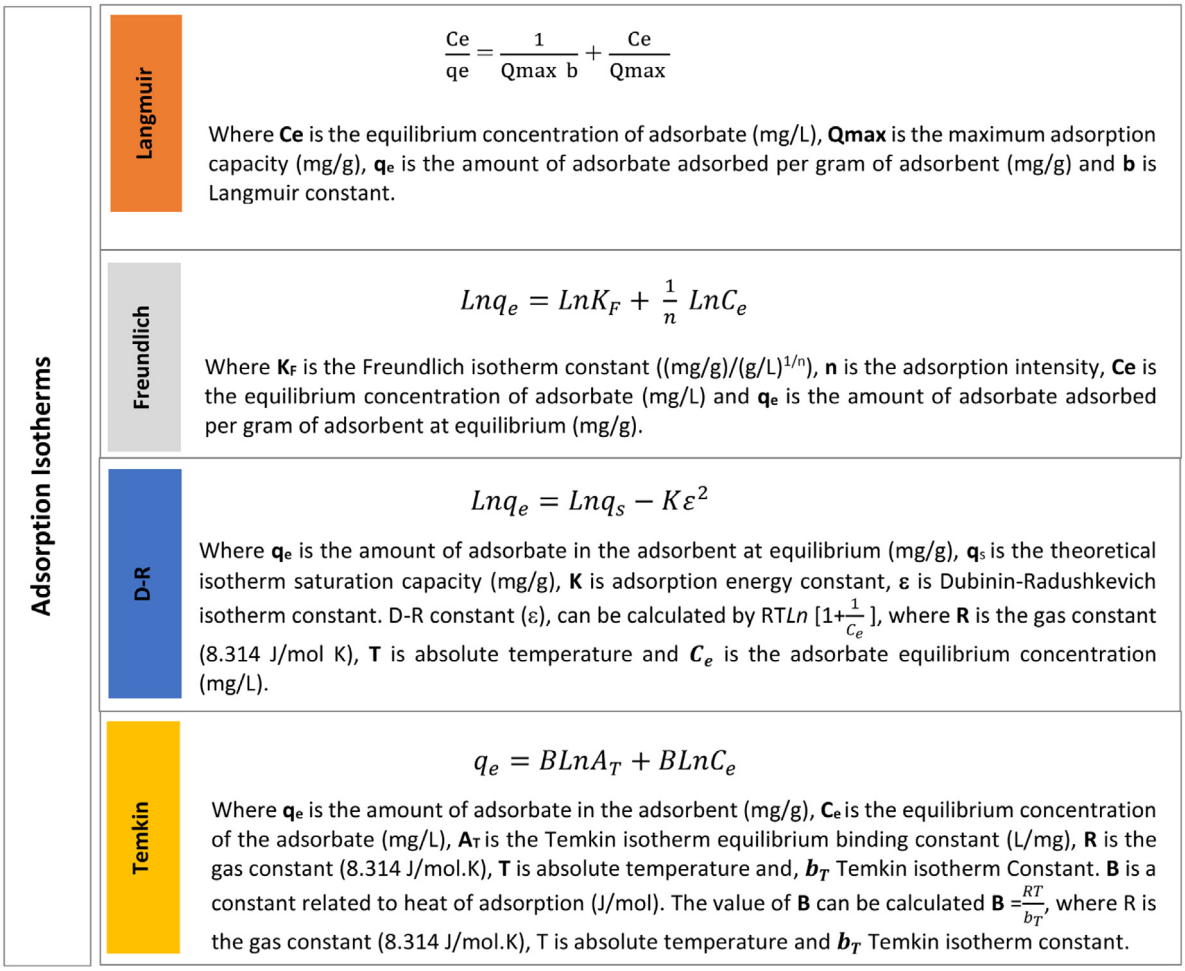

Fig. 2. Adsorption isotherms used in the study and their parameters.

and transmission electron microscopy (TEM). Fourier transform infrared spectroscopy (FT-IR) analysis was performed using (SHIMADZU-IRSpirit) in the range 400 cm $^{-1}$- 4000 cm^{-1}, to determine the surface functional groups of GO and GO-PAA. Energy Dispersive X-ray Analysis (EDX) was done to identify the elemental composition of prepared composites. Raman analysis was also carried out using Thermo fisher scientific DXR Raman Microscope. The Brunauer–Emmett–Teller (BET) analysis using (Quantachrome Corporation, Nova 3000) was carried out to determine the specific surface area of the composites.

2.2.6. Adsorption isotherms

Adsorption isotherms are important curves that provide qualitative information regarding the retention capacity of a given adsorbent (Kecili and Hussain, 2018). These models describe the movement of a substance (adsorbate) from the liquefied medium into the solid medium (adsorbent) at a given temperature and pH (Singh and Susan, 2018). To establish the best-fitted adsorption isotherm, Langmuir adsorption isotherm, Freundlich adsorption isotherm, Temkin isotherm model, and Dubinin-Radushkevich (D-R) adsorption isotherms were used on experimental data. Fig. 2 shows the used adsorption isotherms, their parameters, and equations.

2.2.7. Thermodynamic studies of phenol adsorption

Studying the thermodynamics of adsorption processes is vital for determining the spontaneity of the process. A primary criterion of spontaneity is Gibb's free energy change (ΔG^0). According to this criterion, a spontaneous reaction occurs if ΔG^0 has a negative value at a given temperature. Likewise, changes in entropy ΔS^0 and enthalpy ΔH^0 are essential in

Table 1
Chemical composition (%) of GO and GO-PAA obtained from energy EDX analysis.

Element	Carbon	Oxygen	Silicon	Aluminum	Other	Total	Reference
Graphite	95.47	0.30	1.02	–	3.20	100	Kigozi et al. (2020)
Graphite oxide	69.00	31.00	–	–	–	100	Drewniak et al. (2016)
GO	77.69	17.00	0.30	0.39	4.52	100	Narayan et al. (2018)
GO	68.13	31.70	–	–	0.17	100	Kalil et al. (2018)
GO	44.90	23.59	–	–	31.51	100	Chuah et al. (2020)
GO	53.51	44.65	–	–	1.84	100	Oh and Zhang (2011)
GO	61.26	38.47	0.10	–	0.18	100	Mahesh et al. (2019)
GO	56.02	6.73	–	–	37.25	100	Kigozi et al. (2020)
GO	88.11	11.88	–	–	0.01	100	Siburian et al. (2018)
GO	77.38	14.37	4.94	0.91	2.39	100	**This study**
GO-PAA	73.84	20.03	4.32	1.09	0.72	100	

thermodynamic studies. These parameters could be calculated by equations (3)–(5):

$$\Delta G^0 = -RT \ln\ b \tag{3}$$

$$\Delta G^0 = \Delta H^0 - T\Delta S^0 \tag{4}$$

$$\mathrm{Lb}\ b \frac{\Delta S^0}{R} - \frac{\Delta H^0}{RT} \tag{5}$$

Where R is the gas constant (8.314 J/mol K), T is the temperature in Kelvin (K), and b is the Langmuir constant.

3. Results and discussions

3.1. Characterization of GO and GO-PAA

Fig. 3 shows the TEM images of the GO and GO-PAA. These images show high transparency and low levels of stacking of the GO sheets. In addition to that, the presence of crumples, folds, and wrinkles in the TEM images of GO indicates oxidation and thus, the presence of various oxygen functional (Abu-Nada et al., 2021; Alkhouzaam et al., 2020). The TEM images of GO-PAA also clearly show the presence of (fuzziness) PAA on graphene oxide's surface confirming the polymerization process.

Fig. 4 represents the SEM images of the prepared GO and GO-PAA at various magnifications. Several morphological features such as folds and wrinkles are noted in these images. In addition, the surface appears irregular and rough. Both adsorbents initially look similar, especially at higher magnification since PAA creates a film-like coat on the surface of the GO, and the SEM images do not display structural details. However, at higher magnifications, the polymerization of PAA of GO surface could be somehow noted by the presence of cloud-like material as indicated by an arrow. In addition, the layers of prepared composites have distinguished edges. These layers of graphene at various levels could also be representative of the level of oxidation archived in the preparation of GO (Alkhouzaam et al., 2020).

Energy-dispersive X-ray (EDX) is an analytical method that is utilized for the identification of elemental compositions in the sample. Table 1 and Fig. 5(A) show the chemical composition of GO and GO-PAA based on the energy dispersive X-ray (EDX) analysis. The variations in the percent of oxygen noted in Table 1 are mainly dependent on the level of oxidation, which is consequently dependent on the methodology used for GO preparation. In the current study, it could be noted that the percent of oxygen increased with the PAA modification since PAAs have a carboxyl (C=O) group present on every two carbon atoms of their main chain.

Theoretically, graphene has a large specific surface area (~2620 m^2/g), which signifies its adsorption potential for various organic pollutants (Hu et al., 2015). However, according to this study, GO had a specific surface area of 30.12 m^2/g, and it was reduced to 21.22 m^2/g in GO-PAA. This reduction in surface area after modification coincides with the literature and confirms the successful polymerization of PAA into the surface of the GO (Zhang et al., 2019). Gong et al. (2015) reported that the surface area of GO was 17.87 m^2/g and it was increased to 45.91 m^2/g in the case of modified GO-poly(N-isopropyl acrylamide) (PNIPAM). Whereas Mukherjee et al. (2019) and Li et al. (2012) reported significantly higher surface areas of 312 m^2/g and 305.78 m^2/g respectively. Several phenomena could explain the variation in surface areas of GO composites. First, the BET specific surface area could be as low as 8 m^2/g, possibly due to the stacking of GO layers and agglomeration of GO (Fig. 5(B)), which is a common issue noted when using such composites in aqueous solutions (Pedrosa et al., 2020; Zhang et al., 2020). Additionally, the presence of wrinkling, folding, and crumples on the surface of GO sheets reduces the surface area (Jabari Seresht et al., 2013). The surface area of the generated GO could also be affected by the methodology followed where Esmaeili and Entezari (2014) noticed that oxidation of GO was enhanced with ultrasonic irradiation and the BET surface area was found around 50 m^2/g compared to 30 m^2/g produced when generating GO without ultrasonic irradiation. They noticed that the ultrasonic irradiation led to the introduction of oxygenated functionalities between the layers of graphene, and thus increasing the surface area. Nevertheless, surface

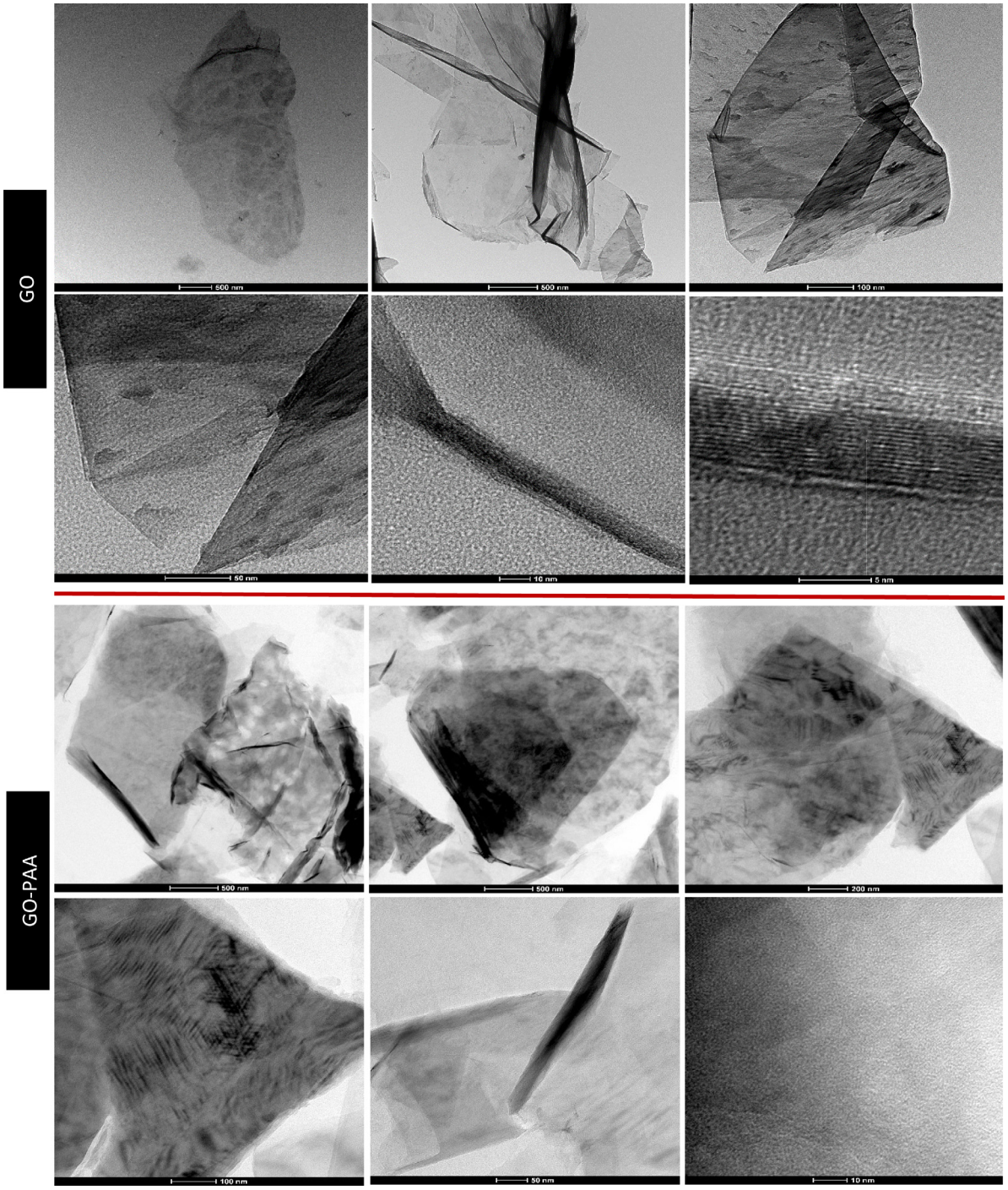

Fig. 3. Transmission electron microscope (TEM) images of GO (top) and GO-PAA (Bottom).

area values that are reported in literature do not always coincide with the level of adsorption as can be noted in Table 2, highlighting the significance of surface modification.

Fig. 6(A) shows the results of the FTIR analysis of GO and GO-PAA. The presence of oxygen groups is verified by the results obtained by the FTIR analysis. This verifies the existence of oxygen-containing groups on the surface of GO. The absorption band at 3405 cm^{-1} is generally attributed to the stretching vibrations of the OH group. The presence of hydroxyl groups is vital for GO surface modification since it serves as a site for the functionalization process (Zhang et al.,

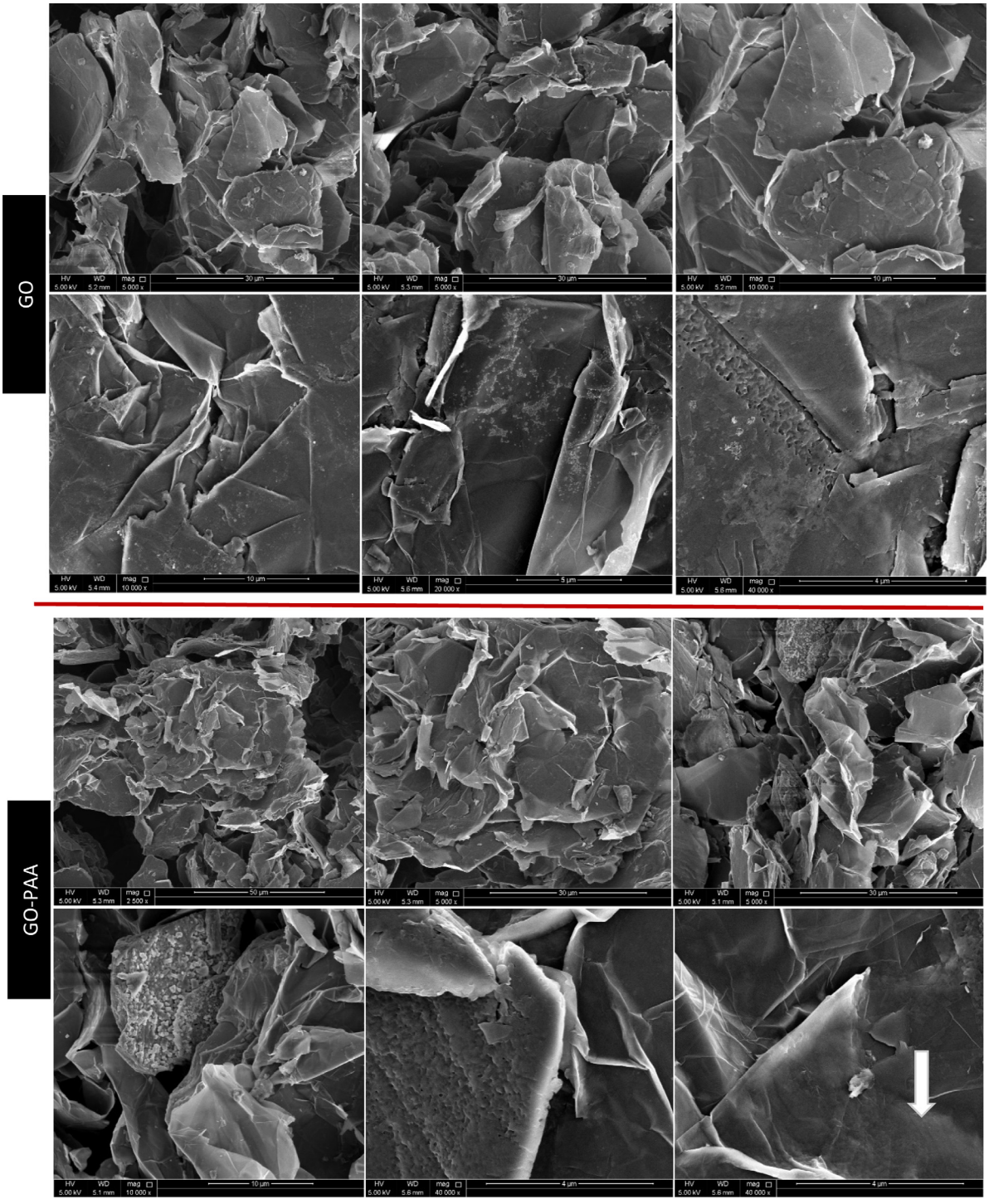

Fig. 4. Scanning electron microscope (SEM) images of GO (top) & GO-PAA (bottom).

2019). The absorption peak at 1764 cm^{-1} and 1566 cm^{-1} could be attributed to the C=O stretching of the carboxyl and carbonyl parts' functional groups.

Fig. 6(B) shows Raman spectrum graphite, GO, and GO-PAA. The (D) peak located at 1355 cm^{-1} is attributed to the breathing mode of sp^2 carbons rings, this is activated by oxygenated functionalities that create defects in graphite's network. On the other hand, the (G) peak located at 1585 cm^{-1} is attributed to the stretching of the bond of the carbon

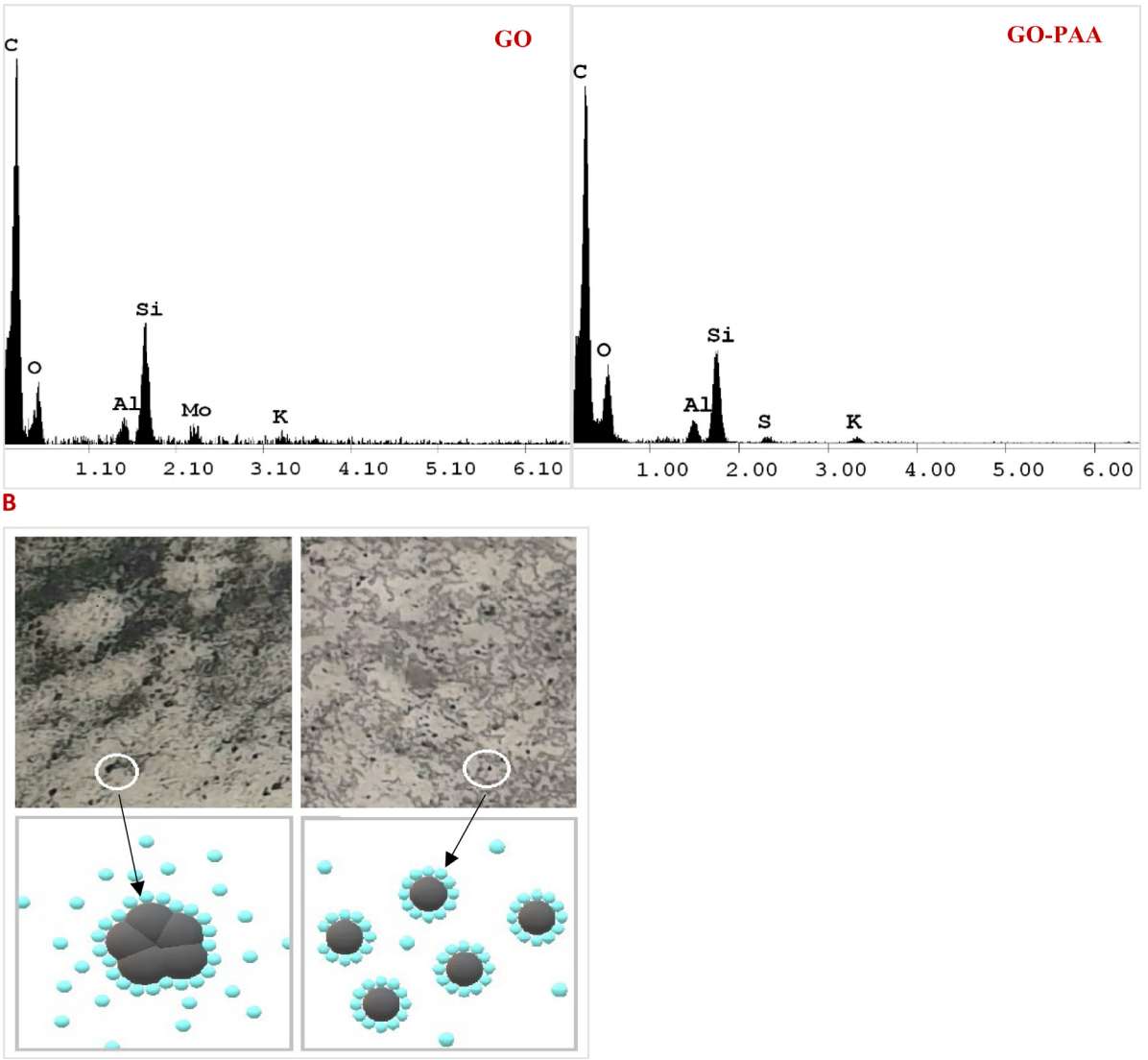

Fig. 5. (A) chemical composition of GO and GO-PAA based on the energy dispersive X-ray (EDX) analysis, and (B) Schematic illustration of phenol adsorption process emphasizing agglomeration GO (left) and dispersion of GO-PAA (right).

pairs in sp ^{2} hybridization. The degree of oxidation could be determined by assessing the relationship between the two bands (D/G) (Ruiz et al., 2019).

3.2. Effect of pH

The pH of any given solution plays an important role in the adsorption process thought changing the net charge of the adsorbent's surface. It can affect the protonation of the functional groups of an adsorbent. Furthermore, it can influence the adsorbate's speciation if it is an ionizable compound. Phenol is an ionizable organic aromatic compound and a weak acid that can exist in aqueous solutions in two forms: dissociated and/or non-dissociated species. The distribution of organic acids and bases in aqueous solutions is highly dependent on the solution's pH and the dissociation constant (pKa). When the pH value is less than the pKa value (which is around 9.8 for phenol (Wu et al., 2014), the dissociated species and the non-dissociated are dominant for organic bases and organic acids, respectively. On the other hand, when pH values are larger than the pKa values, then the dissociated species and the non-dissociated are dominant for organic acids and organic bases respectively (Hu et al., 2015). Thus, the adsorption of organic pollutants is highly dependent on species distribution. If the pH levels are low, then the non-dissociated form will be dominant and thus will be adsorbed easily through $\pi-\pi$ and hydrophobic interactions whereas if the pH levels are high and the pollutants are dissociated (anionic), the $\pi-\pi$ interaction will be weaker, lading to reduced adsorption (Zhang et al., 2013). Due to that, the effect of pH on

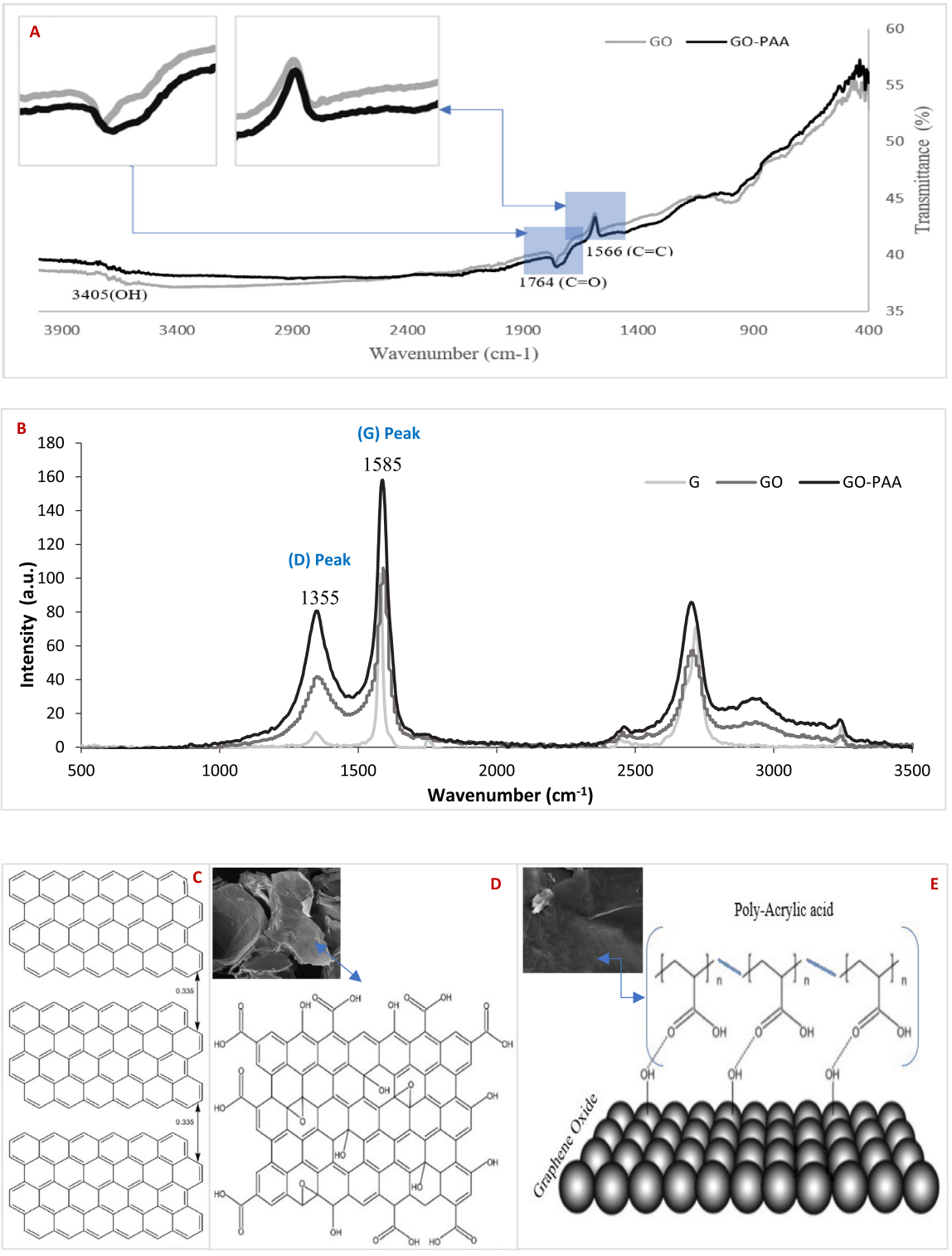

Fig. 6. (A) FT-IR spectra of GO and GO-PAA, (B) Raman spectrum of graphite, GO and GO-PAA, (C) Graphical representation of G, (D) GO, and (E) GO-PAA.

the adsorption of phenol by GO and GO-PAA was investigated, and the results are shown in Fig. 7(A). It is obvious that phenol adsorption by GO and GO-PAA was highly affected by an increase in acidity. In the case of GO, the maximum

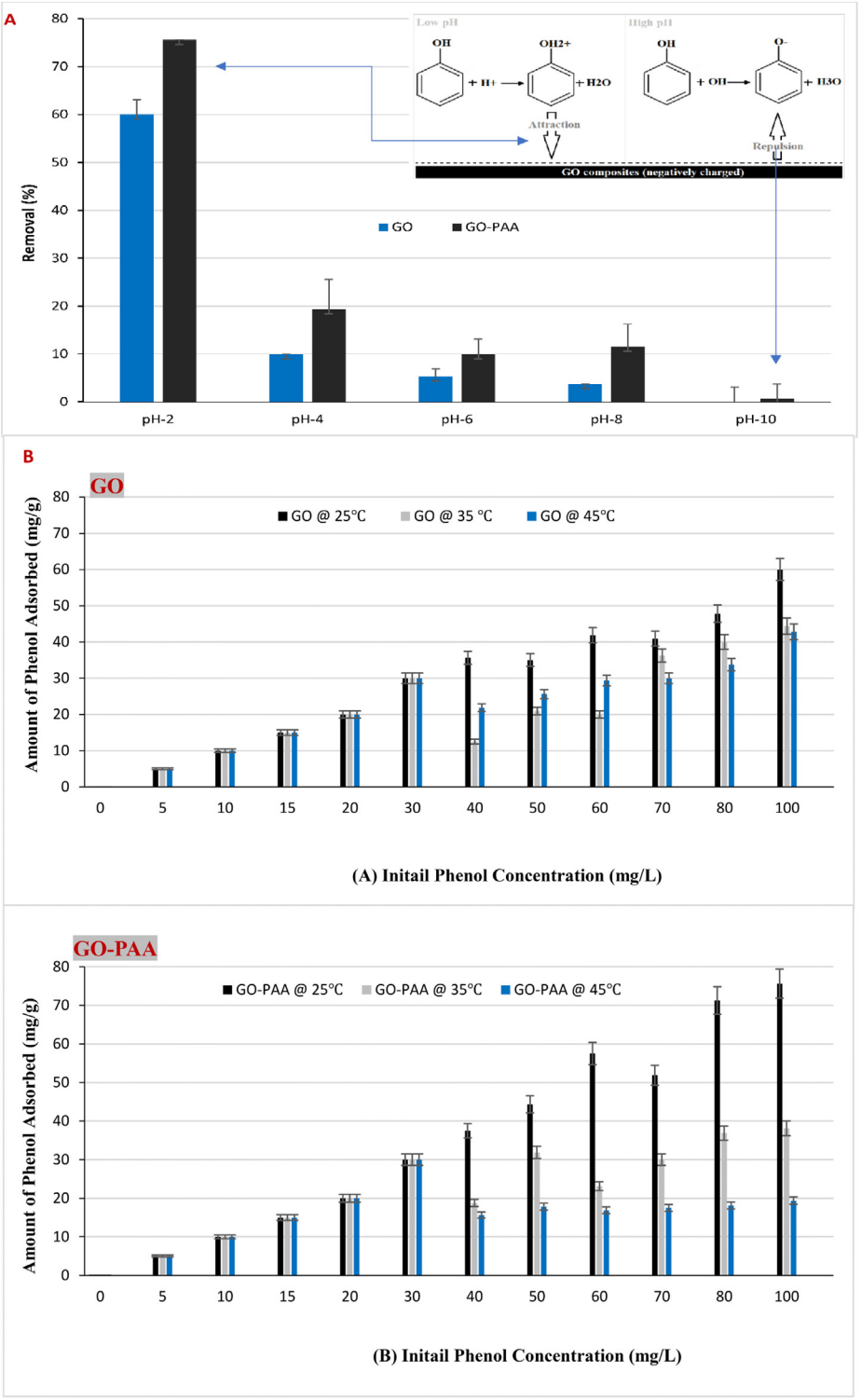

Fig. 7. (A) Removal (%) of phenol from aqueous media using GO and GO-PAA at various pH values. Experimental conditions: initial phenol concentration 100 mg/L; adsorbent's mass 0.02 g; the volume of adsorbate 20 mL; contact time 24 h and temperature 25 °C. Data represent averages of duplicates ± SE and (B) Effect of temperature on phenol adsorption capacities of GO and GO-PAA. Experimental conditions: initial concentrations 0 to 100 mg/L; mass of adsorbent 0.02 g; volume of adsorbate 20 mL; pH 2; and contact time of 24 h.

Table 2
Phenol adsorption capacities of different graphene oxide composites, and Phenol adsorption capacities of various adsorbents.

Phenol adsorption capacities of different graphene oxide composites

Adsorbent	Surface Modification	Adsorption capacity (mg/g)	Experimental Conditions Temp (°C), pH	Adsorbate concentration (mg/L)	BET Surface area (m^2/g)	Isotherm Model	Reference
GO	None	10.23	30, 7	25	312.00	Langmuir	Mukherjee et al. (2019)
GO	None	28.26	25, 6.3	50	305.78	Langmuir/ Freundlich	Li et al. (2012)
GO	None	25.00	–, 7	40	–	Freundlich	Wang et al. (2018a,b)
GO	None	20.20	25, 6	100	–	Langmuir	Al-Ghouti et al. (2022)
GO	None	1.82	35, 7	–	–	Langmuir	Manna et al. (2019)
GO	GO loaded on biochar	23.47	35, 7		–	Langmuir	
GO	PNIPAM	10.00	25, 7	25	45.91	Langmuir	Gong et al. (2015)
TiO_2-TGO	Inorganic	2.09	25, –	100	28.00	Langmuir	Adamu et al. (2016)
TiO_2-TGO	Inorganic	24.00	35, 7.5	100	–	Langmuir	Fu et al. (2016)
GO-PPY	Polymer	201.40	25, 6	20	–	Langmuir	Hu et al. (2015)
NiO@GNCC	MO + O	159.00	25, 10	300	124.92	Langmuir	Wu et al. (2014)
GO	None	48.54	25, 2	100	30.12	Langmuir	This study
GO-PAA	Polymer	84.03	25, 2	100	21.22	Langmuir	

Phenol adsorption capacities of various adsorbents

Adsorbent	Surface Modification	Removal (%)	Adsorption capacity (mg/g)	Experimental conditions Temp (°C), pH	Isotherm Model	Reference
Activated carbon	Magnetic -cobalt	91	107.50	25, 7	Langmuir	Mohammadi et al. (2020)
Activated carbon	Oxidation	80	69.95	20, 5	Freundlich	Sun et al. (2019)
Activated carbon	Heat	–	132.00	15, 7	Langmuir	Lin et al. (2016)
AC (coconut shell)	Heat (900 °C)	–	144.93	25, -	Langmuir	Zhang et al. (2016)
AC (Date pit)	Heat	–	46.08	55, 4	Langmuir	Banat et al. (2004)
Carbon nanotubes	Polyethylene glycol	100	21.23	20,6	Freundlich/ Langmuir	Bin-Dahman and Saleh (2020)
Fly ash	Polydiallydimethyl ammonium chloride	95	13.05	25, 7	Freundlich	Oyehan et al. (2020)
Alumina–zirconia	Calcination	90	83.33	28, 7	Freundlich	Olatubosun et al. (2021)
Bentonite	Surfactant (HDTMA)	–	8.44	25, 6.5	Langmuir/ Freundlich	Alkaram et al. (2009)
Reduced graphene oxide	Nitrogen-doped	99	155.82	30, 6	–	Zhao et al. (2021)
Babul sawdust AC	Heat	83	37.00	30, 6	Redlich–Petersen/ Freundlich	Ingole Ramakant and Lataye Dilip (2015)
Rice husk	Thermally treated	64	–	23, 5.58	–	Daffalla et al. (2020)
Titanium dioxide	–	33	0.44	20, 4.5	Dubinin–Radushkevich	Safwat et al. (2019)
Zeolitic tuff	–	–	34.50	25, -	Freundlich	Yousef et al. (2011)
Activated Biochar	Heat	95	303.00	20, -	Langmuir	Braghiroli et al. (2018)
Miswak root	$KMnO_4$	94	142.20	30, 5	Freundlich	Biglari et al. (2016)
Poplar AC	Pyrolysis	–	625.00	28, -	Langmuir	Hwang et al. (2017)
Ziziphus leaves	–	–	15.00	25, 6	Harkins–Jura	Al Bsoul et al. (2021)
GO	–	47	48.54	25, 2	Langmuir	This study
GO-PAA	PAA	75	84.03	25, 2	Langmuir	

removal of phenol reached (60%) and it was noted at pH 2 with an initial phenol concentration of 100 mg/L. At higher pH levels, there was a decrease in the removal efficiency of phenol, and the removal efficiency was decreased to 10% when pH was increased to 4, and it reached its lowest at pH 10. This could be explained by the fact that when the value of pH is larger than pKa, phenol molecules will dissociate and this leads to the formation of negatively charged anions (Wang et al., 2018a). At such pH levels, the reduction in phenol adsorption could be attributed to the increased electrostatic repulsion between the negative charges of GO composites and the phenolate anions (Hu et al., 2015). Contrary to that, when pH values are less than pKa values, phenol dissociations do not occur, and the adsorption of phenol molecules onto GO happens due to electrostatic interaction and $\pi - \pi$ interactions. In addition, the point of zero charges (PZC) of many graphene oxides/graphite oxides is below pH of 2 (Kosmulski, 2021), this means that at such pH levels, graphene oxides will have equal densities of positive and negative charges on their surface (Rey et al., 2011). Thus, if the working pH values were below the PZC value, the surface charge of the adsorbent would be positive so that the anions can be adsorbed. On the contrary, if the pH is above the PZC value, the surface charge would be negative so that the positively charged molecules with be attracted and adsorbed. Mukherjee et al. (2019) reported that the optimal phenol removal occurred when pH values ranged from 4 to 7. However, when comparing adsorption capacities, it could be noticed that the results are not very different. For example, their reported adsorption capacity was 10.23 mg/g, and in the current study it was noticed that at pH 4, 10% removal was achieved, this corresponds to a capacity of 10 mg/g. On the other hand, phenol adsorption by GO-PAA was also highly increased with acidity, where the maximum removal of phenol (75%) was noted at pH 2. Similar to GO, GO-PAA a decrease in the removal efficiency of phenol was noticed with increased pH

levels, where it reached 19% removal at pH 4 and it reached its lowest (less than 1% removal) at pH 10. Thus, with surface modification, the GO became more dispersible in water as illustrated previously in Fig. 5(B), due to the increased amount or concentration of –COOH groups on the GO surface providing more sites for the donor–acceptor interactions and in turn leading to superior adsorption capacities. These results are similar to a study where GO-PAA was used in the adsorption of gallium ions from water (Zhang et al., 2019). In addition, a recent study where GO was used in phenol adsorption also stated that the highest adsorption occurred at pH 2 (Al-Ghouti et al., 2022). Robati et al. (2016) also reported that GO adsorption of malachite green occurred at lower pH (∼3), highlighting the significance of electrostatic attraction in the removal of organic pollutants (Robati et al., 2016).

3.3. Effect of initial phenol concentration

In the present study, the effect of initial phenol concentration on the adsorption process was examined. The adsorption was increased with increasing phenol concentration, where a 100% removal was observed in initial concentrations from 5 mg/L to 30 mg/L for both GO and GO-PAA. This constant trend was due to the availability of active sites on the surface of the adsorbents, however, when phenol concentration was increased, the availability of sites on the adsorbent's surface was reduced, thus the removal also decreased. Subsequently, the removal efficiency was reduced where it reached about 60% in the case of GO and 75% in the case of GO-PAA with an initial concentration of 100 mg/L. The maximum experimental capacity noticed from the studies of the effect of concentration for the prepared GO reached 47 mg/g at 25 °C and an initial phenol concentration of 80 mg/L, whereas for GO-PAA, the maximum experimental capacity was 75.6 mg/g at 25 °C and with an initial phenol concentration of 100 mg/L. Furthermore, the adsorption capacities of the modified GO-PAA (75.6 mg/g) were higher when compared to GO (47 mg/g) indicating its significance in improving the adsorption capacity of GO by increasing the concentration of surface functional groups. As can be noted in Table 2, the adsorption capacity of the prepared GO was higher than in a study where phenol was adsorbed using where the results of the adsorption capacities were found to be ranging from 1.82 mg/g to 28.26 mg/g (Li et al., 2012; Mukherjee et al., 2019; Wang et al., 2018b). The adsorption capacity of the GO-PAA is higher than in a study where it was found that the maximum adsorption capacity of poly (n-isopropyl acrylamide) modified GO reached (10 mg/g) at the initial phenol concentration of 25 mg/L (Gong et al., 2015). Adamu et al. (2016) and Fu et al. (2016) also reported that GO modified with TiO_2 was able to oxidize phenol in the presence of UV and reported phenol adsorption capacity of 2.09 mg/g and 24.25 mg/g, respectively. Table 2 shows phenol adsorption capacities of various pollutants, ranging from 15 mg/g for Ziziphus leaves and reaching up to 500 mg/g for commercial activated carbon. It could be noticed from the current study that when graphene oxide was used without modification, the adsorption mainly occurred due to $\pi - \pi$ interaction, where the phenol rings stacked and occupied the vacant sites of GO. Whereas after using polyacrylic acid modified GO, the increase in oxygen functionalities on the surface of the adsorbent increased its phenol adsorption capacity due to hydrogen bonding and electronegativity variations between the adsorbent and phenol molecules (Catherine et al., 2018). According to Zhang et al. (2016), the oxygenated functionalities could reduce the π electron density (oxygen atoms will bind to the carbon atoms), leading to reduced $\pi - \pi$ interaction between phenol and GO and thus reduced adsorption of phenol molecules.

3.4. Effect of temperature

To determine the effect of temperature on phenol adsorption by GO and GO-PAA, batch studies were carried out at temperatures 25 °C, 35 °C, and 45 °C, and the results can be seen in Figures 7B and 7C. It is noted for both GO and GO-PAA, the favorable temperature is 25 °C, followed by 35 °C and 45 °C. Generally, when adsorption capacity is decreased with increasing temperature, it means that the adsorption process is exothermic, as in the case of many adsorption studies (Al-Ghouti and Al-Absi, 2020). Many studies on phenol adsorption using GO-based adsorbents also mentioned that the optimum temperature for adsorption was 25 °C, and only a few studies mentioned that temperatures 30 °C and 35 °C were effective in phenol removal as noted in Table 2. Overall, it can be concluded that phenol adsorption by both composites does not favor increased temperatures. This could be due to the increase in diffusion rates of adsorbate through internal and external boundaries of GO pores due to low viscosity (Al-Ghouti et al., 2022). The phenol adsorption capacity was also observed for various adsorbents and temperatures, and it was noted that it fluctuated based on the type of adsorbent used, where some had higher adsorption with increased temperatures, while the other adsorbents reacted differently to temperature and a decrease in adsorption was noticed. For example, several studies on granular activated carbon showed that phenol adsorption capacity decreased with increasing temperatures, whereas phenol adsorption by fly ash reacted differently, and the adsorption increased with increasing temperature in the range of 30 °C to 50 °C (Roostaei and Tezel, 2004).

3.5. Adsorption mechanisms

The adsorption process could be influenced by many factors that involve the adsorbent, the adsorbate, and the experimental conditions as illustrated in Fig. 8(A). An alteration of one could have a significant effect on the entire adsorption process. After the dispersion of graphene-based materials, the efficiency of the adsorption process in removing organic contaminants will depend on several chemical and physical properties as well as electrostatic interactions. The

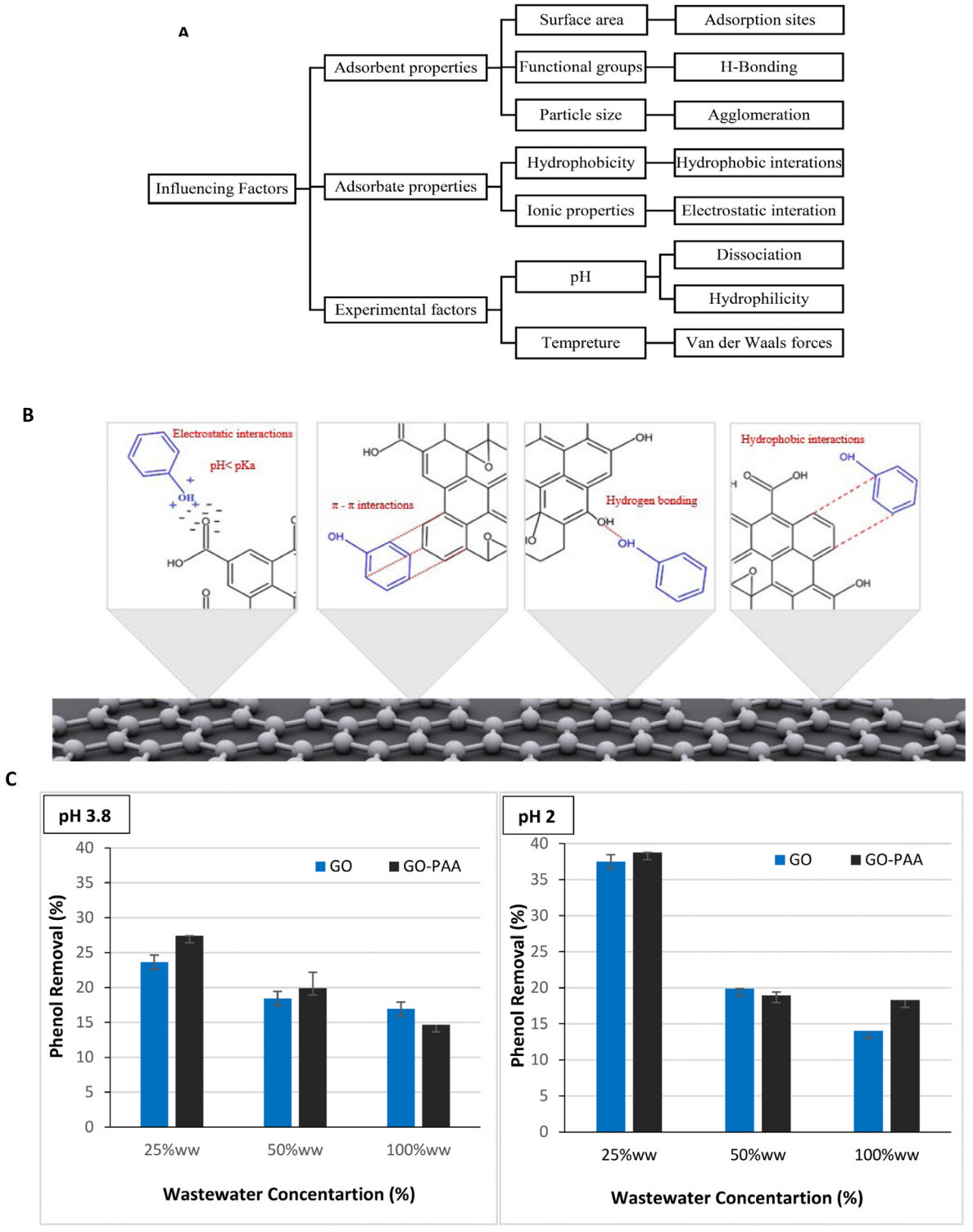

Fig. 8. (A) Factors influencing phenol adsorption into graphene oxide composite, (B). Possible interactions between GO composite and phenol compound, and (C) effects of GO and GO-PAA on phenol adsorption in a real wastewater sample. Experimental conditions: initial concentrations 500 mg/L; the mass of adsorbent 0.02 g; the volume of adsorbate 20 mL; pH 3.8 and 2; temperature 25 °C and contact time 24 h. Data represent averages of duplicates ± SE.

mechanisms involved in adsorption include $\pi-\pi$ interactions, hydrogen bonding, electrostatic interactions, hydrophobic interactions, and dispersion by Van der Waals forces (Catherine et al., 2018; Wang et al. 2018). When phenol molecules and graphene-based adsorbents get interacted in water, the oxygen functionalities on GO's surface will form a bond with the hydrogen from the (OH) of phenol, this interaction can be positively or negatively affected by numerous factors including the type of functional groups, their location, concentration, and surface distribution (Liu et al., 2017). The formation of hydrogen bonds with water molecules makes carbon-based material more hydrophilic and dispersible in the aqueous media and consequently enhances the adsorption of pollutants (Sun et al., 2013). The presence of oxygenated functionalities on the surface of the GO composites played a significant role in the adsorption process as noted from the adsorption capacities of GO and GO-PAA. As it was noticed in this study, the adsorption capacity of GO was 48.54 mg/g, and with surface modification, it increased to 84.03 mg/g at pH 2. This increase could be contributed mainly to the increase of surface oxygen groups even though the surface area was reduced. The resulted difference in charges between the negatively charged GO composites and positively charged phenol molecules resulted in enhanced electrostatic interactions leading to superior adsorption capacity. The dispersion stability was also enhanced with PAA modification as was noticed in the adsorption studies, this is mainly due to the hydrophilicity of AA (Zhang et al., 2019). In addition, $\pi-\pi$ interactions play vital roles in the adsorption process since both phenol and GO have aromatic rings that could stack leading to significant interactions between the two entities in water. Thus, changes in experimental and environmental conditions cause alteration in the interaction mechanisms. Therefore, the presence of multiple mechanisms acting simultaneously is possible as illustrated in Fig. 8(B).

3.6. Adsorption isotherms

Langmuir, Freundlich, Dubinin-Radushkevich (D-R), and Temkin models were all applied to explore the applicability and fitness of these models in the case of GO and GO-PAA and to determine the best fit one. Table 3 and Fig. 9 show the adsorption isotherms and their parameters for GO and GO-PAA. It can be noted that the best-fit model is the Langmuir model for both GO and GO-PAA with correlation coefficient (R^2) values of 0.95 and 0.98, respectively. This indicates that the phenol adsorption occurs in a single layer on the surface of GO and GO-PAA (Catherine et al., 2018) and that there is no transmigration of molecules in the plane of the surface (Hamdaoui and Naffrechoux, 2007). This also suggests that both chemosorption and physisorption adsorption mechanisms should be considered in phenol adsorption studies. Many studies also indicated that the Langmuir model was the best fit for describing phenol adsorption by GO composites. The presence of transparent (non-staked) flat surfaces in the adsorbent supports Langmuir's model since monolayer adsorption requires flat surfaces for uniform adsorption of phenol by $\pi-\pi$ interactions. Furthermore, the affinity between the GO/GO-PAA and phenol could be indicated through the (b) constant values (Al-Ghouti et al., 2019), where the values of b were found higher in the case of GO-PAA compared to the unmodified GO, suggesting that phenol molecules have stronger binding energies to the modified composite. In terms of temperature and adsorption, it was noted that GO had almost constant adsorption capacities in various temperatures, while GO-PAA was strongly affected by temperature, where the adsorption capacity decreased from 84.03mg/g at 25 °C to 21.60 mg/g at 45 °C. On the other hand, the Freundlich isotherm assumes multilayer adsorption, and the obtained removal capacities decreased with increasing temperature. It can be noticed that K_F values for both GO and GO-PAA have decreased with increasing temperature, indicating that adsorption efficiency is reduced. The extent of the exponent (n) obtained from the Freundlich adsorption isotherm can help in indicating the favorability of adsorption. In general, n values in the range (2–10) signify good, (1–2) moderately difficultly, and (<1) poor adsorption characteristics (Hamdaoui and Naffrechoux, 2007). At temperature 25 °C, both GO and GO-PAA have n values of 8.40 and 3.95 respectively, indicating the feasibility of the adsorption process. When n >1, this also corresponds to a physical adsorption process (Al-Ghouti and Al-Absi, 2020). The value ($1/n$) could also be used as an indication of the favorability of adsorption. The ($1/n$) values obtained in this study were 0.12 and 0.25 for GO and GO-PAA respectively, both less than 1, thus indicating favorable adsorption (Mukherjee et al., 2019). The correlation coefficient values obtained from Temkin, and D-R models were low, suggesting they were unable to explain the adsorption process of phenol using GO composites.

3.7. Adsorption thermodynamics

It can be noted from Table 3 that the values of ΔG^0 are negative in all tested temperatures for both GO and GO-PAA indicating that the phenol adsorption process is spontaneous and thermodynamically feasible. Furthermore, it can be noted that at a lower temperature, the ΔG^0 are more negative, indicating a greater driving force to facilitate the adsorption, supporting the previous findings stated in this study, where a significant reduction in adsorption was noted at higher temperatures. Additionally, this observation coincides with the results observed for the adsorption of phenol onto graphene oxide and reduced graphene oxide composites (Al-Ghouti et al., 2022; Wang et al., 2018b). Likewise, the negative values of ΔH^0 for both adsorbents showed that the reactions were exothermic in nature, like most adsorption processes. To a certain extent, physisorption and chemisorption can be classified by the magnitude of enthalpy ΔH^0 and Gibbs free energy ΔG^0. In physisorption, the ΔH^0 is lower than 40 kJ/mol, while in chemisorption the values of ΔH^0 range between 40 and 120 kJ/mol. Whereas for ΔG^0, the change in free energy for physisorption ranges between −20 and 0 kJ/mol, and for chemisorption, its ranges from −80 to −400 kJ/mol (Konicki et al., 2017). In the current study, the

Table 3
The parameters of various isotherms models for phenol adsorption on GO and GO-PAA at 25 °C 35 °C and 45 °C, pH 2, and their thermodynamic parameters.

Isotherms models parameters for phenol adsorption on GO and GO-PAA								
		Langmuir			Freundlich			
	Temp	Qmax (mg/g)	b (dm^3/mg)	R^2	K_F (mg/g)(L/g)^n	n	$1/n$	R^2
	25 °C	48.54	726.70	0.95	28.70	8.40	0.12	0.55
	35 °C	44.84	2010.90	0.45	0.16	0.71	1.45	0.54
	45 °C	50.00	107.16	0.99	6.13	2.25	0.44	0.98
GO		Temkin			Dubinin-Radushkevich (D-R)			
	Temp	A_T (L/mg)	B (J/mol)	R^2	q_s (mg/g)	K	R^2	
	25 °C	266.86	4.81	0.54	41.81	0.00	0.31	
	35 °C	7.87×10^{15}	0.01	0.58	30.73	-6.00×10^{-36}	0.55	
	45 °C	0.34	12.09	0.98	34.55	0.00	0.95	
		Langmuir			Freundlich			
	Temp	Qmax (mg/g)	b (dm^3/mg)	R^2	K_F (mg/g)(L/g)^n	n	$1/n$	R^2
	25 °C	84.03	2508.47	0.98	34.45	3.95	0.25	0.86
	35 °C	52.08	106.36	0.64	9.51	2.86	0.35	0.35
	45 °C	21.60	42.98	0.99	8.89	5.74	0.17	0.97
GO-PAA		Temkin			Dubinin-Radushkevich (D-R)			
	Temp	A_T(L/mg)	B (J/mol)	R^2	q_s (mg/g)	K	R^2	
	25 °C	9.83	13.78	0.85	62.75	0.00	0.59	
	35 °C	2.56	26.99	0.59	33.013	-2.00×10^{-5}	0.21	
	45 °C	6.83	3.02	0.96	18.75	0.00	0.81	

Thermodynamic parameters of phenol adsorption onto GO and GO-PAA					
Adsorbent	Temperature (K)	Ln (b)	ΔG^0 (kJ/mol)	ΔH^0 (kJ/mol)	ΔS^0 (J/mol K)
GO	298	6.59	−16.32	−77.12	0.20
	308	7.61	−19.48		
	318	4.67	−12.36		
GO-PAA	298	7.83	−19.39	−168.56	0.50
	308	4.67	−11.56		
	318	3.76	−9.32		

values of ΔH^0 and ΔG^0 for both dyes were in the range of physisorption; suggesting that adsorption of phenol onto GO composites was driven by a physisorption process. Additionally, the positive ΔS^0 value indicated increased randomness in the solid–liquid interface and affinity of phenol molecules towards GO composites. It could be noted that the ΔG^0 of GO-PAA is more negative than ΔG^0 of the unmodified GO, this could be explained by the structural changes that occurred on the surface of GO-PAA i.e., the addition of carboxyl (C=O) groups, leading to more affinity towards phenol molecules in the aqueous media.

3.8. Effect on real wastewater

The capability of GO and GO-PAA were studied on olive wastewater samples to determine their effectiveness in complex matrices. The phenol concentration in the real olive wastewater reached up to 500 mg/L. These concentrations are five folds of the concentration of synthetic phenol water prepared and used during the study. At pH 2, the maximum removal (%) was noticed at 25% wastewater concentration using GO-PAA, and 39% removal was achieved whereas the unmodified GO achieved 36% removal as noted in Fig. 8(C). In the original wastewater at pH 3.8 (original pH of the sample), the removal efficiency was slightly lower as compared to the pH adjusted samples. It was found that the phenol removal was enhanced by decreasing the pH of the sample, and this was consistent with the batch adsorption studies carried out using synthetic wastewater. It could be noticed that even if the removal (%) from real wastewater was less compared to the synthetic waters, however, the concentration of phenol in these effluents is 5 times higher, thus the removal capacity is consistent in the two types of wastewaters. Moreover, several studies have investigated the adsorptive removal of phenolic compounds from olive mill wastewater (OMW) using various materials. Allaoui et al. (2020) studied the effectiveness of natural clay in the elimination of polyphenols from OMW. It was noted that the maximum adsorption of polyphenols

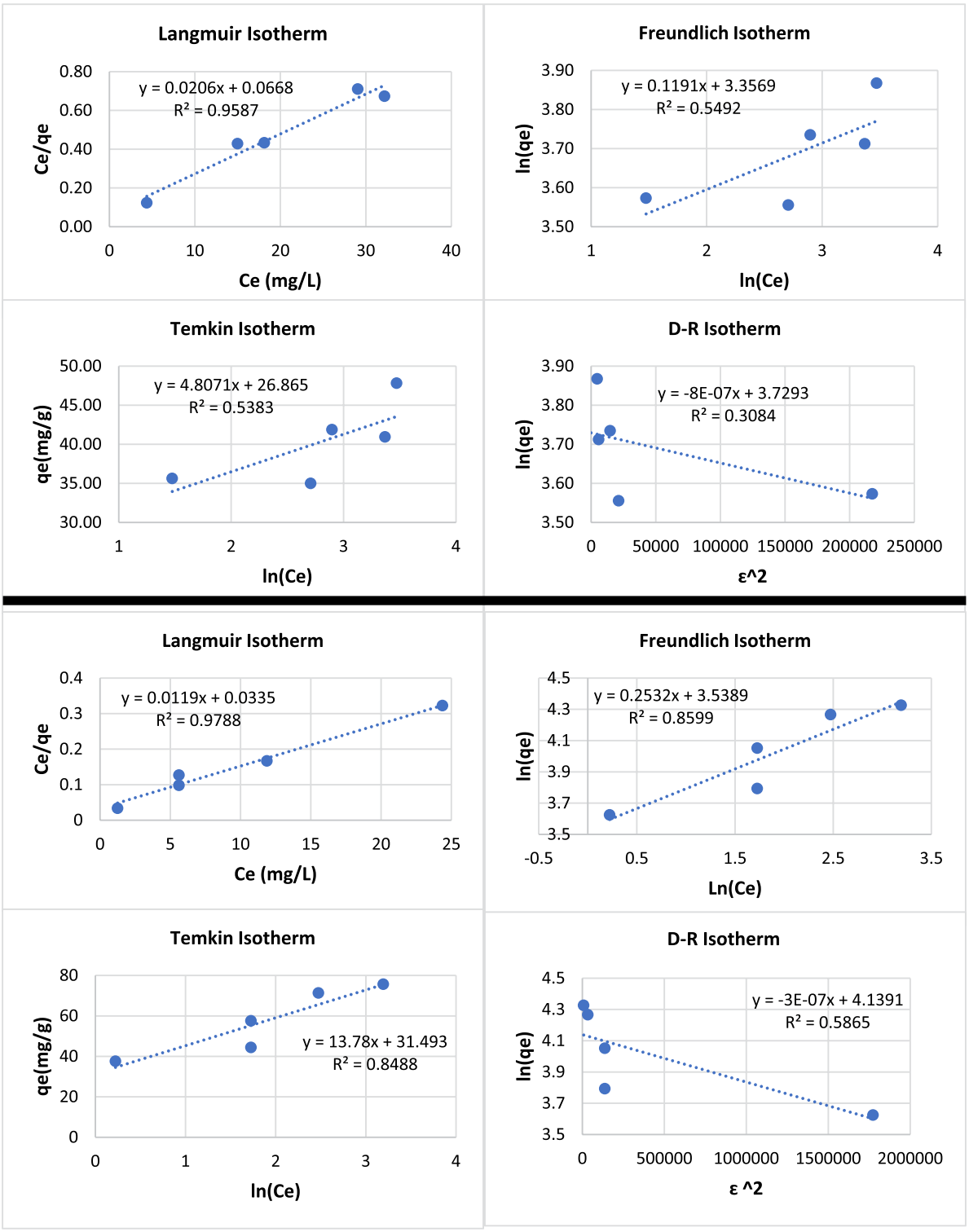

Fig. 9. Adsorption isotherms of GO (top) and GO-PAA (bottom).

occurred at 25 °C and with a capacity of 161 mg/g. On the other hand, Senol et al. (2017) investigated the effectiveness of activated carbons on the removal of bio-phenols from OMW, the results showed that the adsorption capacity reached 65 mg/g at 25 °C. Nassar et al. (2014) investigated the use of magnetic nanoparticles in the treatment of phenols in OMW,

this adsorbent had a capacity of 79.09 mg/g. Activated charcoal and commercial AC had higher adsorption capacities, where the q_{max} reached 390 mg/g and 308 mg/g, respectively (Delgado-Nunez et al., 2009; Eder et al., 2021).

4. Conclusions

The current study was conducted to investigate the performance of GO and GO-PAA composites in the adsorption of phenol from synthetic and real wastewater samples. The highest removal was noted at 25 °C and pH 2 for both adsorbents, and adsorption studies showed that overall, the process did not favor higher temperatures and pH levels. The polyacrylic acid modification increased the adsorption of GO capacity from 48.54 to 84.03 mg/g. In terms of real wastewater treatment, GO and GO-PAA were able to remove 15% and 18% of phenol, respectively under optimum conditions. Furthermore, the adsorption isotherms reviled that the Langmuir isotherm was the best-fitted one in describing the adsorption mechanisms and behaviors. The mechanisms of phenol adsorption on both GO and GO-PAA was mainly dominated by $\pi-\pi$ interactions and the interactions between hydrogen-bond donor and acceptor since the prepared composites had oxygen-carrying functional groups. Additionally, thermodynamic studies reviled that the values of ΔH^0 were −77.12 kJ/mol and −168.56 kJ/mol for GO and GO-PAA respectively, indicating that the adsorption process was spontaneous and of exothermic nature. GO and GO-PAA surface areas of 30.12 m^2/g and 21.22 m^2/g, respectively, however, it was concluded that regardless of surface area, surface modification of GO significantly improved the adsorbent's capacity and dispersibility, especially in acidic conditions, and thus effectively applied for the remediation of phenol-contaminated wastewaters.

CRediT authorship contribution statement

Amina Bibi: Formal analysis, Methodology, Validation, Writing – reviewing and editing. **Shazia Bibi:** Formal analysis, Methodology, Validation, Writing – reviewing and editing. **Mohammed Abu-Dieyeh:** Formal analysis, Methodology, Validation, Writing – reviewing and editing. **Mohammad A. Al-Ghouti:** Conceptualization, Supervision, Visualization, Formal analysis, Methodology, Validation, Writing – reviewing and editing.

Declaration of competing interest

The authors declare that they have no known competing financial interests or personal relationships that could have appeared to influence the work reported in this paper.

Acknowledgment

This report was made possible by Qatar University graduate assistantship program. The statements made herein are solely the responsibility of the author(s).

References

Abu-Nada, A., Abdala, A., McKay, G., 2021. Removal of phenols and dyes from aqueous solutions using graphene and graphene composite adsorption: A review. J. Environ. Chem. Eng. 9 (5), 105858. http://dx.doi.org/10.1016/j.jece.2021.105858.

Adamu, H., Dubey, P., Anderson, J.A., 2016. Probing the role of thermally reduced graphene oxide in enhancing performance of TiO2 in photocatalytic phenol removal from aqueous environments. Chem. Eng. J. 284, 380–388. http://dx.doi.org/10.1016/j.cej.2015.08.147.

Adetayo, A., Runsewe, D., 2019. Synthesis and fabrication of graphene and graphene oxide: A review. Open J. Compos. Mater. 09, 207–229. http://dx.doi.org/10.4236/ojcm.2019.92012.

Al Bsoul, A., Hailat, M., Abdelhay, A., Tawalbeh, M., Al-Othman, A., Al-kharabsheh, I.N., Al-Taani, A.A., 2021. Efficient removal of phenol compounds from water environment using ziziphus leaves adsorbent. Sci. Total Environ. 761, 143229. http://dx.doi.org/10.1016/j.scitotenv.2020.143229.

Al-Ghouti, M.A., Al-Absi, R.S., 2020. Mechanistic understanding of the adsorption and thermodynamic aspects of cationic methylene blue dye onto cellulosic olive stones biomass from wastewater. Sci. Rep. 10 (1), 15928. http://dx.doi.org/10.1038/s41598-020-72996-3.

Al-Ghouti, M.A., Da'ana, D., Abu-Dieyeh, M., Khraisheh, M., 2019. Adsorptive removal of mercury from water by adsorbents derived from date pits. Sci. Rep. 9 (1), 15327. http://dx.doi.org/10.1038/s41598-019-51594-y.

Al-Ghouti, M.A., Sayma, J., Munira, N., Mohamed, D., Da'na, D.A., Qiblawey, H., Alkhouzaam, A., 2022. Effective removal of phenol from wastewater using a hybrid process of graphene oxide adsorption and UV-irradiation. Environ. Technol. Innov. 27, 102525. http://dx.doi.org/10.1016/j.eti.2022.102525.

Aliyev, E., Filiz, V., Khan, M.M., Lee, Y.J., Abetz, C., Abetz, V., 2019a. Structural characterization of graphene oxide: Surface functional groups and fractionated oxidative debris. Nanomaterials (Basel, Switzerland) 9 (8), 1180. http://dx.doi.org/10.3390/nano9081180.

Aliyev, E., Filiz, V., Khan, M.M., Lee, Y.J., Abetz, C., Abetz, V., 2019b. Structural characterization of graphene oxide: Surface functional groups and fractionated oxidative debris. Nanomaterials 9 (8), http://dx.doi.org/10.3390/nano9081180.

Alkaram, U.F., Mukhlis, A.A., Al-Dujaili, A.H., 2009. The removal of phenol from aqueous solutions by adsorption using surfactant-modified bentonite and kaolinite. J. Hard Mater. 169 (1), 324–332. http://dx.doi.org/10.1016/j.jhazmat.2009.03.153.

Alkhouzaam, A., Qiblawey, H., Khraisheh, M., Atieh, M., Al-Ghouti, M., 2020. Synthesis of graphene oxides particle of high oxidation degree using a modified Hummers method. Ceram. Int. 46, 23997–24007. http://dx.doi.org/10.1016/j.ceramint.2020.06.177.

Allaoui, S., Naciri Bennani, M., Ziyat, H., Qabaqous, O., Tijani, N., Ittobane, N., 2020. Kinetic study of the adsorption of polyphenols from olive mill wastewater onto natural clay: Ghassoul. J. Chem. 2020, 7293189. http://dx.doi.org/10.1155/2020/7293189.

Alshabib, M., Onaizi, S.A., 2019. A review on phenolic wastewater remediation using homogeneous and heterogeneous enzymatic processes: Current status and potential challenges. Sep. Purif. Technol. 219, 186–207. http://dx.doi.org/10.1016/j.seppur.2019.03.028.

Azbar, N., Bayram, A., Filibeli, A., Muezzinoglu, A., Sengul, F., Ozer, A., 2004. A review of waste management options in olive oil production. Crit. Rev. Environ. Sci. Technol. 34 (3), 209–247. http://dx.doi.org/10.1080/10643380490279932.

Banat, F., Al-Asheh, S., Al-Makhadmeh, L., 2004. Utilization of raw and activated date pits for the removal of phenol from aqueous solutions. Chem. Eng. Technol. 27 (1), 80–86. http://dx.doi.org/10.1002/ceat.200401868.
Biglari, H., Afsharnia, M., Javan, N., Sajjadi, S.A., 2016. Phenol removal from aqueous solutions by adsorption on activated carbon of Miswak's root treated with KMnO4. Iran. J. Health Sci. 4, 20–30. http://dx.doi.org/10.18869/acadpub.jhs.4.1.20.
Bin-Dahman, O.A., Saleh, T.A., 2020. Synthesis of carbon nanotubes grafted with PEG and its efficiency for the removal of phenol from industrial wastewater. Environ. Nanotechnol. Monitor. Manag. 13, 100286. http://dx.doi.org/10.1016/j.enmm.2020.100286.
Braghiroli, F.L., Bouafif, H., Hamza, N., Neculita, C.M., Koubaa, A., 2018. Production, characterization, and potential of activated biochar as adsorbent for phenolic compounds from leachates in a lumber industry site. Environ. Sci. Pollut. Res. 25 (26), 26562–26575. http://dx.doi.org/10.1007/s11356-018-2712-9.
Catherine, H.N., Ou, M.-H., Manu, B., Shih, Y.-h., 2018. Adsorption mechanism of emerging and conventional phenolic compounds on graphene oxide nanoflakes in water. Sci. Total Environ. 635, 629–638. http://dx.doi.org/10.1016/j.scitotenv.2018.03.389.
Chuah, R., Gopinath, S.C.B., Anbu, P., Salimi, M.N., Yaakub, A.R.W., Lakshmipriya, T., 2020. Synthesis and characterization of reduced graphene oxide using the aqueous extract of Eclipta prostrata. 3 Biotech 10 (8), 364. http://dx.doi.org/10.1007/s13205-020-02365-4.
Daffalla, S.B., Mukhtar, H., Shaharun, M.S., 2020. Preparation and characterization of rice husk adsorbents for phenol removal from aqueous systems. PLoS One 15 (12), http://dx.doi.org/10.1371/journal.pone.0243540.
Das, T.K., Sakthivel, T.S., Jeyaranjan, A., Seal, S., Bezbaruah, A.N., 2020. Ultra-high arsenic adsorption by graphene oxide iron nanohybrid: Removal mechanisms and potential applications. Chemosphere 253, 126702. http://dx.doi.org/10.1016/j.chemosphere.2020.126702.
Delgado-Nunez, M., Richard, D., Schweich, D., 2009. Adsorption of complex phenolic compounds on active charcoal: Adsorption capacity and isotherms. Chem. Eng. J. 148, http://dx.doi.org/10.1016/j.cej.2008.07.023.
Deng, N., Li, M., Zhao, L., Lu, C., de Rooy, S.L., Warner, I.M., 2011. Highly efficient extraction of phenolic compounds by use of magnetic room temperature ionic liquids for environmental remediation. J. Hard Mater. 192 (3), 1350–1357. http://dx.doi.org/10.1016/j.jhazmat.2011.06.053.
Drewniak, S., Muzyka, R., Stolarczyk, A., Pustelny, T., Kotyczka-Morańska, M., Setkiewicz, M., 2016. Studies of reduced graphene oxide and graphite oxide in the aspect of their possible application in gas sensors. Sensors 16 (103), http://dx.doi.org/10.3390/s16010103.
Eder, S., Müller, K., Azzari, P., Arcifa, A., Peydayesh, M., Nyström, L., 2021. Mass transfer mechanism and equilibrium modelling of hydroxytyrosol adsorption on olive pit–derived activated carbon. Chem. Eng. J. 404, 126519. http://dx.doi.org/10.1016/j.cej.2020.126519.
Eigler, S., 2021. Graphene oxide. In: Kobayashi, S., Müllen, K. (Eds.), Encyclopedia of Polymeric Nanomaterials. Springer Berlin Heidelberg, pp. 1–13. http://dx.doi.org/10.1007/978-3-642-36199-9_333-1.
Esmaeili, A., Entezari, M.H., 2014. Facile and fast synthesis of graphene oxide nanosheets via bath ultrasonic irradiation. J. Colloid Interface Sci. 432, 19–25. http://dx.doi.org/10.1016/j.jcis.2014.06.055.
Fakhri, A., 2017. Adsorption characteristics of graphene oxide as a solid adsorbent for aniline removal from aqueous solutions: Kinetics, thermodynamics and mechanism studies. J. Saudi Chem. Soc. 21, S52–S57. http://dx.doi.org/10.1016/j.jscs.2013.10.002.
Fu, C.-C., Juang, R.-S., Huq, M.M., Hsieh, C.-T., 2016. Enhanced adsorption and photodegradation of phenol in aqueous suspensions of titania/graphene oxide composite catalysts. J. Taiwan Inst. Chem. Eng. 67, 338–345. http://dx.doi.org/10.1016/j.jtice.2016.07.043.
Garg, S., Kumar, P., Singh, S., Yadav, A., Dumée, L.F., Sharma, R.S., Mishra, V., 2020. Prosopis juliflora peroxidases for phenol remediation from industrial wastewater — An innovative practice for environmental sustainability. Environ. Technol. Innov. 19, 100865. http://dx.doi.org/10.1016/j.eti.2020.100865.
Gholami-Bonabi, L., Ziaefar, N., Sheikhloie, H., 2020. Removal of phenol from aqueous solutions by magnetic oxide graphene nanoparticles modified with ionic liquids using the taguchi optimization approach. Water Sci. Technol. 81 (2), 228–240. http://dx.doi.org/10.2166/wst.2020.082.
Gong, Z., Li, S., Han, W., Wang, J., Ma, J., Zhang, X., 2015. Recyclable graphene oxide grafted with poly(N-isopropylacrylamide) and its enhanced selective adsorption for phenols. Appl. Surf. Sci. 362, http://dx.doi.org/10.1016/j.apsusc.2015.11.251.
Hamdaoui, O., Naffrechoux, E., 2007. Modeling of adsorption isotherms of phenol and chlorophenols onto granular activated carbon: Part I. Two-parameter models and equations allowing determination of thermodynamic parameters. J. Hard Mater. 147 (1), 381–394. http://dx.doi.org/10.1016/j.jhazmat.2007.01.021.
Hamdi, M., 1993. Future prospects and constraints of olive mill wastewaters use and treatment: A review. Bioprocess Eng. 8 (5), 209–214. http://dx.doi.org/10.1007/BF00369831.
Hu, R., Dai, S., Shao, D., Alsaedi, A., Ahmad, B., Wang, X., 2015. Efficient removal of phenol and aniline from aqueous solutions using graphene oxide/polypyrrole composites. J. Molecular Liquids 203, 80–89. http://dx.doi.org/10.1016/j.molliq.2014.12.046.
Hur, J., Shin, J., Yoo, J., Seo, Y.-S., 2015. Competitive adsorption of metals onto magnetic graphene oxide: Comparison with other carbonaceous adsorbents. Sci. World J. 2015, 836287. http://dx.doi.org/10.1155/2015/836287.
Hwang, H., Sahin, O., Choi, J., 2017. Manufacturing a super-active carbon using fast pyrolysis char from biomass and correlation study on structural features and phenol adsorption. RSC Adv. 7, 42192–42202. http://dx.doi.org/10.1039/C7RA06910C.
Ingole Ramakant, S., Lataye Dilip, H., 2015. Adsorptive removal of phenol from aqueous solution using activated carbon prepared from babul sawdust. J. Hazard. Toxic Radioact. Waste 19 (4), 04015002. http://dx.doi.org/10.1061/(ASCE)HZ.2153-5515.0000271.
Jabari Seresht, R., Jahanshahi, M., Rashidi, A., Ghoreyshi, A.A., 2013. Synthesize and characterization of graphene nanosheets with high surface area and nano-porous structure. Appl. Surf. Sci. 276, 672–681. http://dx.doi.org/10.1016/j.apsusc.2013.03.152.
Jiménez, S., Micó, M.M., Arnaldos, M., Medina, F., Contreras, S., 2018. State of the art of produced water treatment. Chemosphere 192, 186–208. http://dx.doi.org/10.1016/j.chemosphere.2017.10.139.
Kalil, H., Maher, S., Bose, T., Bayachou, M., 2018. Manganese oxide/hemin-functionalized graphene as a platform for peroxynitrite sensing. J. Electrochem. Soc. 165, G3133–G3140. http://dx.doi.org/10.1149/2.0221812jes.
Kecili, R., Hussain, C.M., 2018. Chapter 4 - mechanism of adsorption on nanomaterials. In: Hussain, C.M. (Ed.), Nanomaterials in Chromatography. Elsevier, pp. 89–115. http://dx.doi.org/10.1016/B978-0-12-812792-6.00004-2.
Kigozi, M., Koech, R.K., Kingsley, O., Ojeaga, I., Tebandeke, E., Kasozi, G.N., Onwualu, A.P., 2020. Synthesis and characterization of graphene oxide from locally mined graphite flakes and its supercapacitor applications. Results Mater. 7, 100113. http://dx.doi.org/10.1016/j.rinma.2020.100113.
Kissi, M., Mountadar, M., Assobhei, O., Gargiulo, E., 2001. Roles of two white-rot basidiomycete fungi in decolorisation and detoxification of olive mill waste water. Appl. Microbiol. Biotechnol. 57, 221–226. http://dx.doi.org/10.1007/s002530100712.
Konicki, W., Aleksandrzak, M., Mijowska, E., 2017. Equilibrium, kinetic and thermodynamic studies on adsorption of cationic dyes from aqueous solutions using graphene oxide. Chem. Eng. Res. Des. 123, 35–49. http://dx.doi.org/10.1016/j.cherd.2017.03.036.
Kosmulski, M., 2021. The pH dependent surface charging and points of zero charge. IX. Update. Adv. Colloid Interface Sci. 296, 102519.
Li, Y., Du, Q., Liu, T., Sun, J., Jiao, Y., Xia, Y., et al., 2012. Equilibrium, kinetic and thermodynamic studies on the adsorption of phenol onto graphene. Mater. Res. Bull. 47 (8), 1898–1904. http://dx.doi.org/10.1016/j.materresbull.2012.04.021.
Li, Z., Sellaoui, L., Luiz Dotto, G., Bonilla-Petriciolet, A., Ben Lamine, A., 2019. Understanding the adsorption mechanism of phenol and 2-nitrophenol on a biopolymer-based biochar in single and binary systems via advanced modeling analysis. Chem. Eng. J. 371, 1–6. http://dx.doi.org/10.1016/j.cej.2019.04.035.
Lin, J.Q., Yang, S.E., Duan, J.M., Wu, J.J., Jin, L.Y., Lin, J.M., Deng, Q.L., 2016. The adsorption mechanism of modified activated carbon on phenol. MATEC Web Conf. 67, http://dx.doi.org/10.1051/matecconf/20166703040.

Liu, L., Tan, S., Horikawa, T., Do, D.D., Nicholson, D., Liu, J., 2017. Water adsorption on carbon - A review. Adv. Colloid Interface Sci. 250, 64–78. http://dx.doi.org/10.1016/j.cis.2017.10.002.
Mahesh, V., Zahari, A., Rashmi, W., Khalid, M., Priyanka, J., 2019. Synthesis and characterization of hybrid graphene oxide/gold nanoparticle.
Mandeep, Gulati A., Kakkar, R., 2020. Graphene-based adsorbents for water remediation by removal of organic pollutants: Theoretical and experimental insights. Chem. Eng. Res. Des. 153, 21–36. http://dx.doi.org/10.1016/j.cherd.2019.10.013.
Manna, S., Prakash, S., Das, P., 2019. Synthesis of graphene oxide nano-materials coated bio-char using carbonaceous industrial waste for phenol separation from water. Colloids Surf. A 581, 123818. http://dx.doi.org/10.1016/j.colsurfa.2019.123818.
Mohamad Said, K.A., Ismail, A.F., Abdul Karim, Z., Abdullah, M.S., Hafeez, A., 2021. A review of technologies for the phenolic compounds recovery and phenol removal from wastewater. Process Saf. Environ. Prot. 151, 257–289. http://dx.doi.org/10.1016/j.psep.2021.05.015.
Mohamed, A., Yousef, S., Nasser, W.S., Osman, T.A., Knebel, A., Sánchez, E.P.V., Hashem, T., 2020. Rapid photocatalytic degradation of phenol from water using composite nanofibers under UV. Environ. Sci. Eur. 32 (1), 160. http://dx.doi.org/10.1186/s12302-020-00436-0.
Mohammadi, S.Z., Darijani, Z., Karimi, M.A., 2020. Fast and efficient removal of phenol by magnetic activated carbon-cobalt nanoparticles. J. Alloys Compd. 832, 154942. http://dx.doi.org/10.1016/j.jallcom.2020.154942.
Molla, A., Li, Y., Mandal, B., Kang, S.G., Hur, S.H., Chung, J.S., 2019. Selective adsorption of organic dyes on graphene oxide: Theoretical and experimental analysis. Appl. Surf. Sci. 464, 170–177. http://dx.doi.org/10.1016/j.apsusc.2018.09.056.
Mukherjee, M., Goswami, S., Banerjee, P., Sengupta, S., Das, P., Banerjee, P.K., Datta, S., 2019. Ultrasonic assisted graphene oxide nanosheet for the removal of phenol containing solution. Environ. Technol. Innov. 13, 398–407. http://dx.doi.org/10.1016/j.eti.2016.11.006.
Mulinacci, N., Romani, A., Galardi, C., Pinelli, P., Giaccherini, C., Vincieri, F.F., 2001. Polyphenolic content in olive oil waste waters and related olive samples. J. Agricult. Food Chem. 49 (8), 3509–3514. http://dx.doi.org/10.1021/jf000972q.
Narayan, P.S., Teradal, N.L., Jaldappagari, S., Satpati, A.K., 2018. Eco-friendly reduced graphene oxide for the determination of mycophenolate mofetil in pharmaceutical formulations. J. Pharmaceut. Anal. 8 (2), 131–137. http://dx.doi.org/10.1016/j.jpha.2017.12.001.
Nassar, N.N., Arar, L.A., Marei, N.N., Abu Ghanim, M.M., Dwekat, M.S., Sawalha, S.H., 2014. Treatment of olive mill based wastewater by means of magnetic nanoparticles: Decolourization, dephenolization and COD removal. Environ. Nanotechnol. Monit. Manag. 1–2, 14–23. http://dx.doi.org/10.1016/j.enmm.2014.09.001.
Oh, W.-C., Zhang, F.-J., 2011. Preparation and characterization of graphene oxide reduced from a mild chemical method. Asian J. Chem. 23 (2), 875–879.
Olatubosun, O.Dare., Okoronkwo, A.E., Odewole, O.A., Olumayowa Oluwasola, H., Balogun, A.A., Akpomie, K.G., 2021. Phenolic compounds removal from aqueous solution by composite of alumina-zirconia. Int. J. Environ. Anal. Chem. 1–21. http://dx.doi.org/10.1080/03067319.2021.1928103.
Oyehan, T.A., Olabemiwo, F.A., Tawabini, B.S., Saleh, T.A., 2020. The capacity of mesoporous fly ash grafted with ultrathin film of polydiallyldimethyl ammonium for enhanced removal of phenol from aqueous solutions. J. Cleaner Prod. 263, 121280. http://dx.doi.org/10.1016/j.jclepro.2020.121280.
Pedrosa, M., Da Silva, E.S., Pastrana-Martínez, L.M., Drazic, G., Falaras, P., Faria, J.L., et al., 2020. Hummers' and Brodie's graphene oxides as photocatalysts for phenol degradation. J. Colloid Interface Sci. 567, 243–255. http://dx.doi.org/10.1016/j.jcis.2020.01.093.
Rahmanian, N., Jafari, S., Galanakis, C., 2014. Recovery and removal of phenolic compounds from olive mill wastewater. J. Oil Fat Ind. 91, 1–18. http://dx.doi.org/10.1007/s11746-013-2350-9.
Rey, A., Zazo, J., Casas, J., Bahamonde, A., Rodriguez, J., 2011. Influence of the structural and surface characteristics of activated carbon on the catalytic decomposition of hydrogen peroxide. Appl. Catalysis A 402 (1–2), 146–155.
Robati, D., Rajabi, M., Moradi, O., Najafi, F., Tyagi, I., Agarwal, S., Gupta, V.K., 2016. Kinetics and thermodynamics of malachite green dye adsorption from aqueous solutions on graphene oxide and reduced graphene oxide. J. Molecular Liquids 214, 259–263. http://dx.doi.org/10.1016/j.molliq.2015.12.073.
Roostaei, N., Tezel, F.H., 2004. Removal of phenol from aqueous solutions by adsorption. J. Environ. Manag. 70 (2), 157–164. http://dx.doi.org/10.1016/j.jenvman.2003.11.004.
Ruiz, S., Tamayo, J., Ospina, J., Navia-Porras, D., Valencia Zapata, M., Mina, J., Tovar, C., 2019. Antimicrobial films based on nanocomposites of chitosan/poly(vinyl alcohol)/graphene oxide for biomedical applications. Biomolecules 9, 109. http://dx.doi.org/10.3390/biom9030109.
Safwat, S.M., Medhat, M., Abdel-Halim, H., 2019. Adsorption of phenol onto aluminium oxide and zinc oxide: A comparative study with titanium dioxide. Sep. Sci. Technol. 54 (17), 2840–2852. http://dx.doi.org/10.1080/01496395.2018.1549572.
Sajid, M., Hussain, J., Iqbal, M., Abbas, Z., Hussain, I., Baig, M.A., 2018. Assessing the generation, recycling and disposal practices of electronic/electrical-waste (EWaste) from major cities in Pakistan. Waste Manag. 84, 394–401.
Saleh, T.A., Elsharif, A.M., Asiri, S., Mohammed, A.-R.I., Dafalla, H., 2020. Synthesis of carbon nanotubes grafted with copolymer of acrylic acid and acrylamide for phenol removal. Environ. Nanotechnol. Monit. Manag. 14, 100302. http://dx.doi.org/10.1016/j.enmm.2020.100302.
Senol, A., Hasdemir, İ.M., Hasdemir, B., Kurdaş, İ., 2017. Adsorptive removal of biophenols from olive mill wastewaters (OMW) by activated carbon: mass transfer, equilibrium and kinetic studies. Asia-Pac. J. Chem. Eng. 12 (1), 128–146. http://dx.doi.org/10.1002/apj.2060.
Shi, Y.-C., Wang, A.-J., Wu, X.-L., Chen, J.-R., Feng, J.-J., 2016. Green-assembly of three-dimensional porous graphene hydrogels for efficient removal of organic dyes. J. Colloid Interface Sci. 484, 254–262. http://dx.doi.org/10.1016/j.jcis.2016.09.008.
Siburian, R., Sihotang, H., Raja, S., Supeno, M., Simanjuntak, C., 2018. New route to synthesize of graphene nano sheets. Orient. J. Chem. 34, 182–187. http://dx.doi.org/10.13005/ojc/340120.
Singh, N.B., Susan, A.B.H., 2018. 21 - Polymer nanocomposites for water treatments. In: Jawaid, M., Khan, M.M. (Eds.), Polymer-Based Nanocomposites for Energy and Environmental Applications. Woodhead Publishing, pp. 569–595. http://dx.doi.org/10.1016/B978-0-08-102262-7.00021-0.
Solomakou, N., Goula, A.M., 2021. Treatment of olive mill wastewater by adsorption of phenolic compounds. Rev. Environ. Sci. Biotechnol. 20 (3), 839–863. http://dx.doi.org/10.1007/s11157-021-09585-x.
Soto-Hernandez, M., Palma Tenango, M., García-Mateos, M., 2017. Phenolic Compounds - Natural Sources, Importance and Applications. http://dx.doi.org/10.5772/67213.
Sun, J., Liu, X., Zhang, F., Zhou, J., Wu, J., Alsaedi, A., et al., 2019. Insight into the mechanism of adsorption of phenol and resorcinol on activated carbons with different oxidation degrees. Colloids Surf. A 563, 22–30. http://dx.doi.org/10.1016/j.colsurfa.2018.11.042.
Sun, Y., Yang, S., Zhao, G., Wang, Q., Wang, X., 2013. Adsorption of polycyclic aromatic hydrocarbons on graphene oxides and reduced graphene oxides. Chem. – Asian J. 8 (11), 2755–2761. http://dx.doi.org/10.1002/asia.201300496.
Terao, K., 2021. Poly(acrylic acid) (PAA). In: Kobayashi, S., Müllen, K. (Eds.), Encyclopedia of Polymeric Nanomaterials. Springer Berlin Heidelberg, pp. 1–6. http://dx.doi.org/10.1007/978-3-642-36199-9_279-1.
Thakur, K., Kandasubramanian, B., 2019. Graphene and graphene oxide-based composites for removal of organic pollutants: A review. J. Chem. Eng. Data 64 (3), 833–867. http://dx.doi.org/10.1021/acs.jced.8b01057.
Tong, S.W., Loh, K.P., 2014. 3.22 - Graphene properties and application. In: Sarin, V.K. (Ed.), Comprehensive Hard Materials. Elsevier, pp. 565–583. http://dx.doi.org/10.1016/B978-0-08-096527-7.00059-3.
US-EPA, 2014. Priority Pollutant List.
Wang, X., Hu, Y., Min, J., Li, S., Deng, X., Yuan, S., Zuo, X., 2018a. Adsorption characteristics of phenolic compounds on graphene oxide and reduced graphene oxide: A batch experiment combined theory calculation. Appl. Sci. 8, 1950. http://dx.doi.org/10.3390/app8101950.

Wang, X., Hu, Y., Min, J., Li, S., Deng, X., Yuan, S., Zuo, X., 2018b. Adsorption characteristics of phenolic compounds on graphene oxide and reduced graphene oxide: a batch experiment combined theory calculation. Appl. Sci. 8 (10), 1950.
Wu, Y., Luo, H., Wang, H., Zhang, L., Liu, P., Feng, L., 2014. Fast adsorption of nickel ions by porous graphene oxide/sawdust composite and reuse for phenol degradation from aqueous solutions. J. Colloid Interface Sci. 436, 90–98. http://dx.doi.org/10.1016/j.jcis.2014.08.068.
Xie, B., Qin, J., Wang, S., Li, X., Sun, H., Chen, W., 2020. Adsorption of phenol on commercial activated carbons: Modelling and interpretation. Int. J. Environ. Res. Public Health 17 (3), 789. http://dx.doi.org/10.3390/ijerph17030789.
Yousef, R.I., El-Eswed, B., Al-Muhtaseb, A.a.H., 2011. Adsorption characteristics of natural zeolites as solid adsorbents for phenol removal from aqueous solutions: Kinetics, mechanism, and thermodynamics studies. Chem. Eng. J. 171 (3), 1143–1149. http://dx.doi.org/10.1016/j.cej.2011.05.012.
Zhang, D., Huo, P., Liu, W., 2016. Behavior of phenol adsorption on thermal modified activated carbon. Chin. J. Chem. Eng. 24 (4), 446–452. http://dx.doi.org/10.1016/j.cjche.2015.11.022.
Zhang, Y., Liu, X., Wang, Y., Lou, Z., Shan, W., Xiong, Y., 2019. Polyacrylic acid-functionalized graphene oxide for high-performance adsorption of gallium from aqueous solution. J. Colloid Interface Sci. 556, http://dx.doi.org/10.1016/j.jcis.2019.08.032.
Zhang, Y., Tang, Y., Li, S., Yu, S., 2013. Sorption and removal of tetrabromobisphenol A from solution by graphene oxide. Chem. Eng. J. 222, 94–100. http://dx.doi.org/10.1016/j.cej.2013.02.027.
Zhang, S., Wang, H., Liu, J., Bao, C., 2020. Measuring the specific surface area of monolayer graphene oxide in water. Mater. Lett. 261, 127098. http://dx.doi.org/10.1016/j.matlet.2019.127098.
Zhao, R., Li, Y., Ji, J., Wang, Q., Li, G., Wu, T., Zhang, B., 2021. Efficient removal of phenol and p-nitrophenol using nitrogen-doped reduced graphene oxide. Colloids Surf. A 611, 125866. http://dx.doi.org/10.1016/j.colsurfa.2020.125866.